NASA TECHNICAL NOTE

NASA TN D-2346

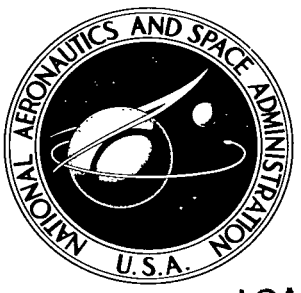




# LOW-SPEED LONGITUDINAL AERODYNAMIC INVESTIGATION OF PARAWINGS AS AUXILIARY LIFTING DEVICES FOR A SUPERSONIC AIRPLANE CONFIGURATION

*by W. Pelham Phillips*

*Langley Research Center*
*Langley Station, Hampton, Va.*

NATIONAL AERONAUTICS AND SPACE ADMINISTRATION • WASHINGTON, D. C. • JULY 1964

# LOW-SPEED LONGITUDINAL AERODYNAMIC INVESTIGATION OF PARAWINGS AS AUXILIARY LIFTING DEVICES FOR A SUPERSONIC AIRPLANE CONFIGURATION

By W. Pelham Phillips

Langley Research Center
Langley Station, Hampton, Va.

NATIONAL AERONAUTICS AND SPACE ADMINISTRATION

For sale by the Office of Technical Services, Department of Commerce,
Washington, D.C. 20230 -- Price $1.50

# LOW-SPEED LONGITUDINAL AERODYNAMIC INVESTIGATION OF PARAWINGS AS AUXILIARY LIFTING DEVICES FOR A SUPERSONIC AIRPLANE CONFIGURATION

By W. Pelham Phillips
Langley Research Center

## SUMMARY

A wind-tunnel investigation has been conducted to determine the improvement in low-speed aerodynamic performance characteristics which might be realized by the use of high-performance parawings as auxiliary lifting surfaces for overloaded supersonic airplanes. Included in the investigation were the effects of parawing orientation with respect to the airplane on the longitudinal trim characteristics in overloaded cruise conditions (at moderate lift coefficients).

Studies of the effects of varying parawing incidence angle and vertical position relative to the airplane indicated that the addition of auxiliary parawings can produce maximum lift-drag ratios similar in magnitude to that of the airplane-alone configuration and at lift coefficients nearly three times as large.

The drag penalty generally encountered in providing longitudinal trimming moments at moderate lift coefficients was reduced by using longitudinal parawing position to trim the configurations at maximum lift-drag ratio. Slightly larger values of trimmed maximum lift-drag ratio could then be obtained for the airplane-parawing configuration having a parawing incidence of $5^{\circ}$ than for the airplane-alone configuration using conventional methods of trim.

Increasing the parawing incidence to $10^{\circ}$ provides more linear pitching-moment variation with lift in the high-lift range; this enables the use of control deflections for trim at the higher lifts desirable for take-off or landing. However, this increase in parawing incidence results in a reduction in maximum aerodynamic efficiency.

## INTRODUCTION

The National Aeronautics and Space Administration is investigating methods of improving the low-speed performance potential of supersonic aircraft in an overloaded or high-altitude flight condition. Improved low-speed performance for overloaded tactical aircraft would enhance the subsonic range capability and

reduce take-off and landing distances; this would allow the aircraft to assume additional roles of long-range ferry or aerial reconnaissance.

One means of providing the desired overload or altitude capability might be through the use of flexible auxiliary wings (parawings) that could be easily attached to structurally adaptable aircraft for these special missions. The results of an exploratory study of a parawing as a high-lift device for aircraft are reported in reference 1. The conventional low-aspect-ratio conical parawing used, although providing improvements in high-lift capability, is not entirely suitable for long-range ferry or aerial-reconnaissance missions since its addition results in a notable reduction in the maximum aerodynamic efficiency from that of the airplane-alone configuration. Recent studies (ref. 2) directed towards improving the performance of parawings have indicated that considerable improvement can be accomplished by the use of cylindrical-type (zero camber and twist) canopies rather than the conventional conical canopies which have extreme washout, and by the use of higher aspect ratio.

The purpose of this paper, therefore, is to report the results of a low-speed wind-tunnel investigation of the longitudinal aerodynamic characteristics of a supersonic airplane configuration utilizing high-performance auxiliary parawings having both rigid and flexible leading edges. Several methods of attaching the parawing to the airplane were investigated. Also investigated were the effects of parawing orientation with respect to the airplane on the longitudinal trim characteristics in overloaded subsonic cruise conditions (moderate lift coefficients). For this study horizontal-tail deflections were used to attain trim at the high lifts required for landing or take-off. Wind-tunnel studies were made in the Langley high-speed 7- by 10-foot tunnel at a free-stream dynamic pressure of 8 pounds per square foot corresponding to an average test Reynolds number based on the mean aerodynamic chord of the airplane model wing of $0.585 \times 10^6$. The test angle-of-attack range extended from approximately $-1^\circ$ to $24^\circ$ at a sideslip angle of $0^\circ$.

## SYMBOLS

The data herein are presented about the stability system of axes. All coefficients including the data obtained for the parawing alone are nondimensionalized with respect to the projected planform area and mean aerodynamic chord of the airplane model wing. The moment reference point was located at 67.1 percent of the fuselage length for all configurations except the parawing-alone configuration for which the moment reference point was located at 70 percent of the parawing root chord.

$C_L$ lift coefficient, $\frac{\text{Lift}}{qS_w}$

$C_D$ drag coefficient, $\frac{\text{Drag}}{qS_w}$

$C_m$ pitching-moment coefficient, $\frac{\text{Pitching moment}}{qS_w\bar{c}_w}$

A aspect ratio

c local chord, in.

$\bar{c}_w$ mean aerodynamic chord (airplane model), 14.625 in.

$h_p$ vertical distance of parawing angle-of-attack pivot above moment reference point, in.

$\delta_t$ horizontal-tail deflection, deg

$l_p$ longitudinal distance of parawing angle-of-attack pivot fore (negative) and aft (positive) of moment reference point, in.

q free-stream dynamic pressure, lb/sq ft

$S_p$ parawing planform area, 2.82 sq ft

$S_w$ wing planform area (airplane model), 3.190 sq ft

$\alpha$ angle of attack, deg

$i_p$ parawing incidence angle (angle between parawing keel and model reference plane), deg

$\Lambda$ leading-edge sweep angle, deg

L/D lift-drag ratio

$(L/D)_{max}$ maximum lift-drag ratio

t thickness, in.

Subscripts:

p geometric characteristics pertinent to parawing

trim trimmed value

Model components:

A airplane model

$P_1$ strut-supported rigid leading-edge parawing with spreader bar

$P_2$ strut-supported rigid leading-edge parawing without spreader bar and with cables connecting parawing and model wing tips

$P_3$ cable-supported rigid leading-edge parawing

$P_4$ strut-supported flexible leading-edge parawing with cables connecting parawing and model wing tips

## WIND-TUNNEL MODELS

The wind-tunnel models represented a twin-engine supersonic attack airplane having various auxiliary parawing configurations deployed above the fuselage and wing. Pertinent details of the configurations are shown in figure 1. Photographs of several configurations investigated are shown as figure 2. A complete description of the airplane model may be found in reference 3, wherein it is designated configuration IV.

Each of the auxiliary parawing models had identical geometric characteristics as defined by the flat pattern of the canopy membranes ($A_p = 6.07$, $\Lambda_p = 48.25°$, and $S_p = 2.82$ square feet). The rigid leading-edge panels of parawings $P_1$, $P_2$, and $P_3$ were constructed from 1/32-inch-thick aluminum sheet to simulate the degree of flexibility considered structurally feasible for full-scale parawings. The panel cross sections normal to the parawing leading edge resemble a figure six. The section reference points formed a right cylindrical helix which had a radius of 28.02 inches and a helix angle of 48.25°. The reference points at the root and tips formed a plane with the center line of the parawing keel, and the average leading-edge sweep angle (projected) was 49°. The membrane of parawings $P_1$, $P_2$, and $P_3$ was a tightly woven nylon rip-stop sailcloth weighing 1.40 ounces per square yard.

Four different methods were utilized in attaching the rigid leading-edge parawings to the airplane model (fig. 1(b)). Parawing $P_1$ was mounted on several unswept struts of varying lengths which positioned the parawing pivot axis at heights of 3.70, 6.35, 11.05, and 20.65 inches above the model reference plane. The keel of parawing $P_1$ could also be mounted directly to the fuselage which fixed the pivot axis at a height of 1.38 inches. An unswept spreader bar constructed from streamlined tubing ($t/c = 0.425$) connected the leading-edge panels to the keel at about 75 percent of the root chord.

The longitudinal location of the support struts was variable so that the parawing pivot axis could be moved in 1-inch increments from 2.2 inches ahead to 1.8 inches aft of the moment reference point (center of gravity) of the airplane model.

Parawing $P_2$ was supported at the keel by the same struts as were utilized for parawing $P_1$; however, no spreader bar was used. The parawing tips were connected to the airplane model wing tips by 1/32-inch-diameter braided steel cables.

The geometry of parawing $P_3$ was identical to parawing $P_2$, the only configuration difference being the means of attachment. This parawing configuration was attached to the model fuselage as well as the wing tips by 1/32-inch-diameter cable.

The flexible leading-edge parawing $P_4$ was formed from tightly woven dacron sailcloth weighing 3.8 ounces per square yard. The leading edge was simply a length of 1/8-inch-diameter nylon parachute cord covered by 1/4-inch-diameter plastic tubing (fig. 1(b)). The shortest support strut ($h_p$ = 3.70 in.) was utilized and the parawing tip leading and trailing edges were attached to the model wing tips by the nylon cord.

## TESTS AND CORRECTIONS

The investigation was conducted in the Langley high-speed 7- by 10-foot tunnel at a free-stream dynamic pressure of 8 pounds per square foot. The average Reynolds number of the investigation was $0.585 \times 10^6$ based on the mean aerodynamic chord of the airplane model wing. The models were sting-mounted to reduce support interference and were tested through an angle-of-attack range from about $-1^\circ$ to $24^\circ$. A six-component strain-gage balance was used to measure the forces and moments acting on the airplane model.

The drag data were adjusted to correspond to free-stream static conditions at the model base. Also, the internal duct drag was measured and subtracted from the total drag. The angle of attack has been corrected to account for the combined deflection of the balance and sting-support system under load.

The parawing-alone test results have been corrected for the wind-on tares of the balance and adapter since they were located just below the parawing keel, although no attempt was made to correct the data for the interference effects of the parawing-balance combination. No attempt was made to fix transition on either the parawing or airplane model surfaces.

## RESULTS AND DISCUSSION

A comparison of drag characteristics for the various-length parawing support struts used in the wind-tunnel investigation is presented in figure 3. Longitudinal aerodynamic characteristics for the airplane model alone and parawing configuration $P_1$ alone are shown in figure 4. The basic longitudinal aerodynamic characteristics for the airplane-parawing configurations are presented in figures 5 to 13. Longitudinal trim characteristics for the configurations are summarized in figures 14 to 18. An index for the figures is presented as table I. All coefficients are based on the geometric characteristics of the basic airplane wing.

A comparison of the aerodynamic characteristics of the basic airplane configuration (fig. 4(a)) with those of the isolated parawing (fig. 4(b)) indicates

that the lift-drag ratio of the parawing alone is nearly twice that of the basic airplane alone and occurs at approximately twice the lift coefficient and at an angle of attack approximately 5° higher. In general, the results obtained with the parawing in combination with the airplane indicate that the lift coefficient for maximum lift-drag ratio can be nearly tripled with little or no loss in the magnitude of the maximum lift-drag ratio. Because of the difference in angle-of-attack requirements, interference effects between the airplane and the parawing, and stability and control requirements, the investigation included the effects of parawing incidence and vertical and longitudinal position relative to the airplane. A brief summary of these effects is presented in the following paragraphs.

Successive increases in the vertical distance of the parawing above the airplane center of gravity are noted to result in increased lift coefficients for maximum untrimmed lift-drag ratio and increases in L/D in the higher lift-coefficient range (fig. 5). Increasing the separation distance between the parawing and the airplane center of gravity (from $h_p$ = 3.70 to 11.05 inches) results in a reduction in adverse interference effects at moderate to high angles of attack as indicated by the successive increases in lift and reductions in drag due to lift. Further increasing the support length $h_p$ from 11.05 to 20.65 inches provides only minor improvements in L/D in the high-lift range. Because of this and the question of structural feasibility of a full-scale support strut corresponding to the 20.65-inch strut, no further data for parawing configurations mounted on the large strut were obtained.

A comparison of the effects of varying the parawing incidence angle (fig. 6) indicates that the highest values of lift-drag ratio from moderate to high lifts (including $(L/D)_{max}$) are attained for a parawing keel angle of approximately 5°. The variation of pitching moment with lift for this keel angle exhibited a more pronounced tendency towards instability at high lifts than was shown for the other keel angles investigated. The instabilities noted restrict the magnitude of the usable trimmed lift coefficients, for most configurations having $i_p = 5°$, to values less than 1.3 (fig. 18). However, these lift coefficients are considerably higher than those for the configuration without the parawing. The magnitude of the unstable trend would indicate that it is amenable to aerodynamic fixes on the airplane wing since the instability is characteristic of the airplane-alone configuration.

Moving the parawing pivot forward of the airplane center of gravity provided longitudinal trimming moments with only slight reductions in lift-drag ratios. As noted in figure 9(b) for configuration $AP_1$ with $h_p$ = 6.35 inches and $i_p = 5°$, moving the parawing pivot approximately 2 inches forward of the center of gravity ($l_p$ = -0.20 to $l_p$ = -2.20) provided a trimmed $(L/D)_{max}$ of 7.00 as opposed to the untrimmed value of about 7.24. This is, of course, due to the absence of any appreciable trim-drag penalty since longitudinal movements of the auxiliary wing rather than conventional control surface deflections were used in attaining trim characteristics. However, the 2-inch forward movement of the parawing pivot does provide a reduction of approximately $0.05\bar{c}_w$ in the low-lift longitudinal stability levels of the parawing configurations having $i_p = 5°$.

Since fore and aft movements of the parawing configurations produced only small effects on the lift-drag ratios, a summary of the lift-drag ratios and pitching moments for configurations having strut-supported rigid leading-edge auxiliary parawings is presented in figures 14 to 17 for the parawing longitudinal positioning necessary to trim the various configurations near $(L/D)_{max}$ without the use of any control deflections. Also included are the effects of horizontal-tail deflection on the longitudinal trim characteristics at high lifts.

A summary of the trimmed lift-drag ratios and angles of attack for trim as a function of lift coefficient for configurations having the strut-supported rigid leading-edge auxiliary parawings is presented in figure 18. The results indicate that a trimmed lift-drag ratio somewhat greater than that for the airplane without the parawing could be obtained with an auxiliary parawing located at $h_p = 6.35$ and $l_p = -2.20$ with $i_p = 5^\circ$ and that it occurred at a lift coefficient approximately three times that for the airplane-alone configuration.

Increasing the parawing keel angle to $10^\circ$ also linearizes the pitching-moment curve at high lifts (compare figs. 15(a) and (b)). Configuration $AP_1$ having $i_p = 10^\circ$ and employing variable deflections of the horizontal tails is noted in figure 18 to attain values of trimmed lift coefficients of about 1.4 without exceeding allowable ground clearance angles for the configuration ($\alpha \approx 14^\circ$). However, using a $10^\circ$ keel angle results in a reduction in maximum aerodynamic efficiency in the moderate lift range.

Since provision for in-flight parawing orientation changes would increase the complexity and structural weight of the support system, it would appear practical to incorporate the capability for preflight longitudinal positioning and keel-angle orientation in the design of parawing supports to allow the preferred parawing orientations for missions specifying either overloaded optimum cruise or short-field landings.

## SUMMARY OF RESULTS

A wind-tunnel investigation has been conducted to determine the improvement in low-speed aerodynamic performance characteristics which might be realized by the use of high-performance parawings as auxiliary lifting surfaces for overloaded supersonic airplanes. Results of the investigation may be summarized as follows:

1. Studies of the effects of varying parawing incidence and vertical position relative to the airplane indicated that the addition of auxiliary parawings can produce maximum lift-drag ratios similar in magnitude to that of the airplane-alone configuration and at lift coefficients nearly three times as large.

2. The drag penalty generally encountered in providing longitudinal trimming moments at moderate lift coefficients was reduced by using longitudinal parawing position to trim the configurations at maximum lift-drag ratio.

Slightly larger values of trimmed maximum lift-drag ratio could then be obtained for the airplane-parawing configuration having a parawing incidence of $5^{\circ}$ than for the airplane-alone configuration using conventional methods of trim.

3. Increasing the parawing incidence angle to $10^{\circ}$ provides more linear pitching-moment variation with lift in the high-lift range; this enables the use of control deflections for trim at the higher lifts desirable for take-off or landing. However, this increase in parawing incidence results in a reduction in maximum aerodynamic efficiency.

Langley Research Center,
National Aeronautics and Space Administration,
Langley Station, Hampton, Va., February 29, 1964.

## REFERENCES

1. Naeseth, Rodger L.: An Exploratory Study of a Parawing as a High-Lift Device for Aircraft. NASA TN D-629, 1960.

2. Polhamus, Edward C., and Naeseth, Rodger L.: Experimental and Theoretical Studies of the Effects of Camber and Twist on the Aerodynamic Characteristics of Parawings Having Nominal Aspect Ratios of 3 and 6. NASA TN D-972, 1963.

3. Polhamus, Edward C., Alford, William J., Jr., and Foster, Gerald V.: Subsonic and Supersonic Aerodynamic Characteristics of an Airplane Configuration Utilizing Double-Pivot Variable-Sweep Wings. NASA TM X-743, 1962.

TABLE I.- INDEX FOR DATA FIGURES

| Configuration | $h_p$, in. | $l_p$, in. | $i_p$, deg | $\delta_t$, deg | Figure |
|---|---|---|---|---|---|
| $AP_1$ | 3.70, 6.35, 11.05, 20.65 | -0.20 | 5 | 0 | 5 |
| | 6.35 | -0.20 | 0, 5, 10, 15, 25 | ↓ | 6 |
| | 1.38 | -0.20 | 0 | | 7 |
| | 6.35 | -2.20, -0.20, 1.80 | 0 | | 8(a) |
| | 11.05 | -2.20, -0.20, 1.80 | 0 | | 8(b) |
| | 1.38 | -2.20, -1.20, -0.20 | 5 | | 9(a) |
| | 6.35 | -2.20, -1.20, -0.20, 0.80, 1.80 | 5 | | 9(b) |
| | 11.05 | -2.20, -1.20, -0.20, 0.80, 1.80 | 5 | | 9(c) |
| | 6.35 | -2.20, -1.20, -0.20, 0.80, 1.80 | 10 | | 10(a) |
| | 11.05 | -2.20, -1.20, -0.20, 0.80, 1.80 | 10 | | 10(b) |
| $AP_2$ | 6.35 | -2.20, -1.20, -0.20 | 5 | 0 | 11(a) |
| | 6.35 | -0.20, 1.80 | 10 | 0 | 11(b) |
| $AP_3$ | 6.35 | 0.30, 0.80, 1.80 | 5, 10, 15 | 0 | 12 |
| $AP_4$ | 3.70 | -1.20 | 5, 10 | 0 | 13 |
| A, $AP_1$ | 1.38 | -2.20 | 5 | 0, -5, -10 | 14 |
| | 6.35 | -2.20 | 5 | ↓ | 15(a) |
| | 6.35 | -0.20 | 10 | | 15(b) |
| | 11.05 | -2.20 | 5 | | 16(a) |
| | 11.05 | -0.20 | 10 | | 16(b) |
| A, $AP_2$ | 6.35 | -2.20 | 5 | 0, -5, -10 | 17(a) |
| | 6.35 | -0.20 | 10 | 0, -5, -10 | 17(b) |
| A, $AP_1$, $AP_2$, $AP_3$, $AP_4$ | 1.38, 3.70, 6.35, 11.05 | -2.20, -1.20, -0.20, 0.80 | 5, 10 | Variable | 18 |

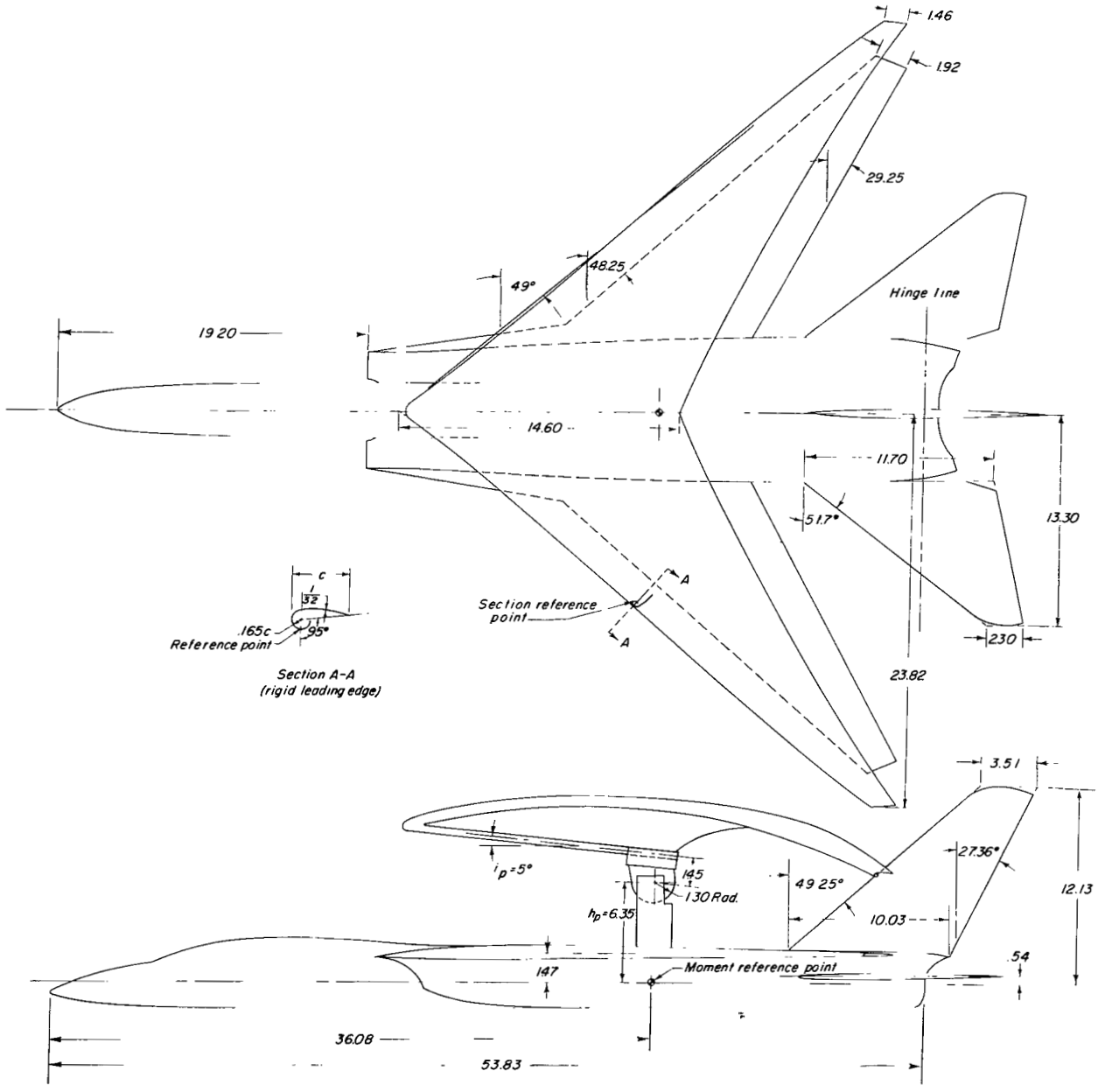


(a) Configuration $AP_1$. $i_p = 5^o$; $h_p = 6.35$ in.; $l_p = -0.20$ in.

Figure 1.- Geometric characteristics of the airplane-parawing configurations of the investigation. All linear dimensions are in inches.

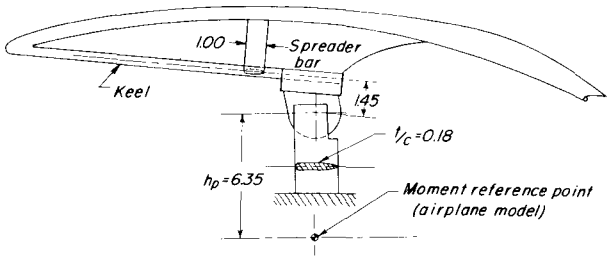


Parawing $P_1$

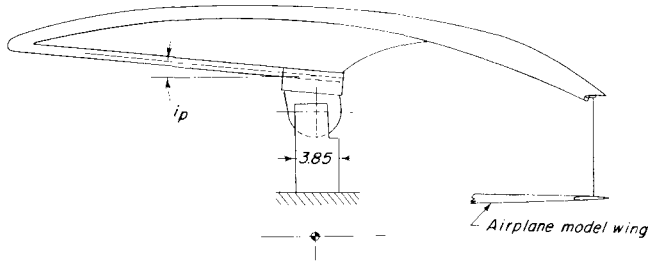


Parawing $P_2$

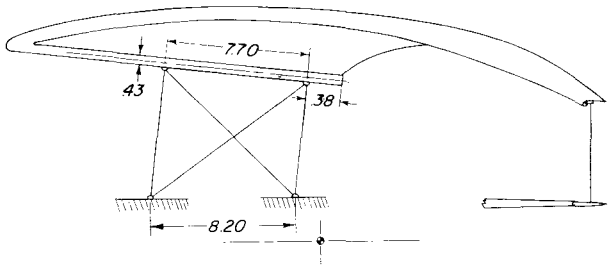


Parawing $P_3$

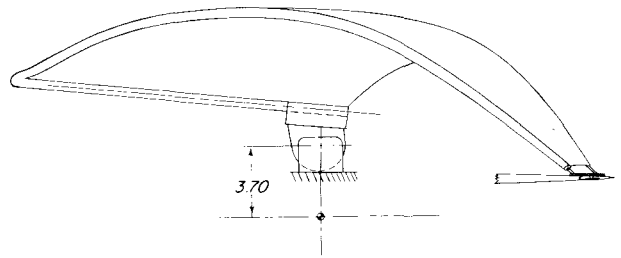


Parawing $P_4$

(b) Parawing configurations $P_1$, $P_2$, $P_3$, and $P_4$.

Figure 1.- Concluded.

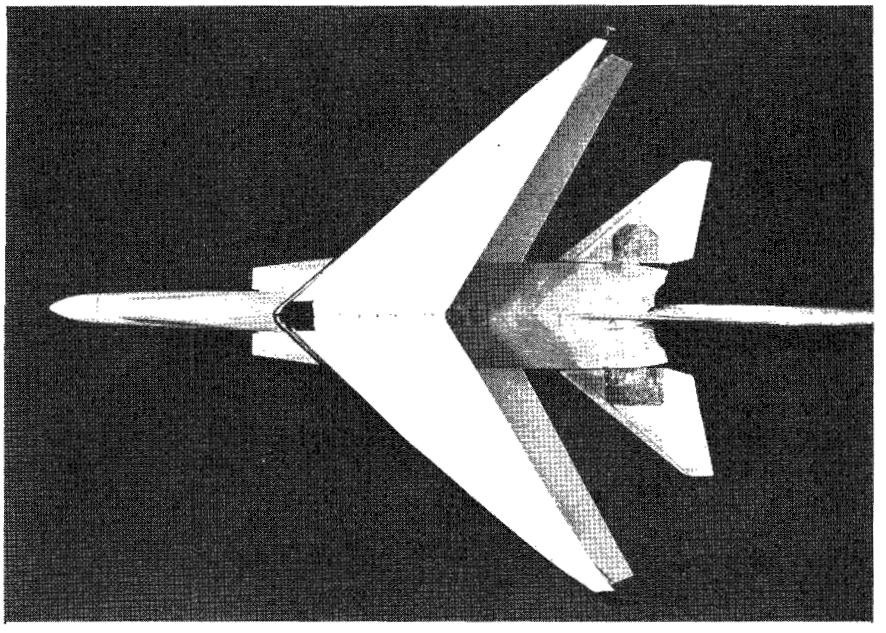

L-62-6743

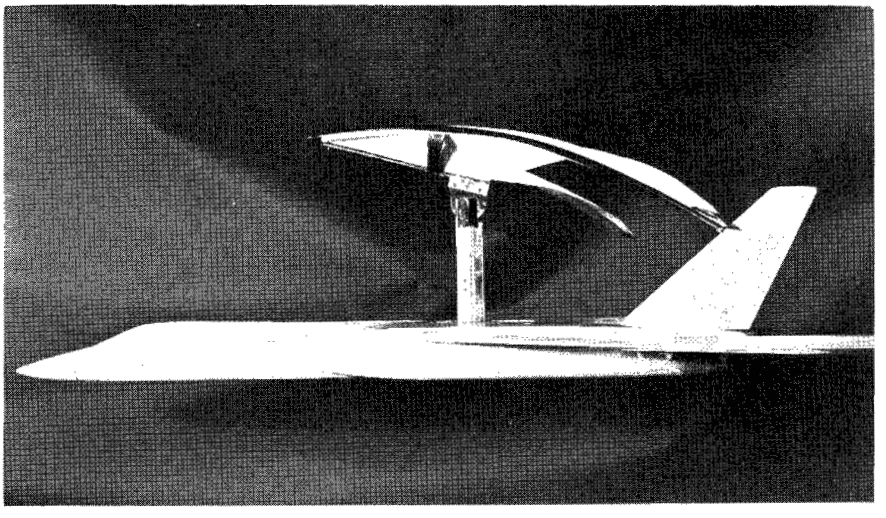

L-62-6744

(a) Configuration $AP_1$. $h_p$ = 11.05 in.; $l_p$ = -2.20 in.; $i_p$ = 15°.

Figure 2.- Several of the parawing-airplane configurations studied.

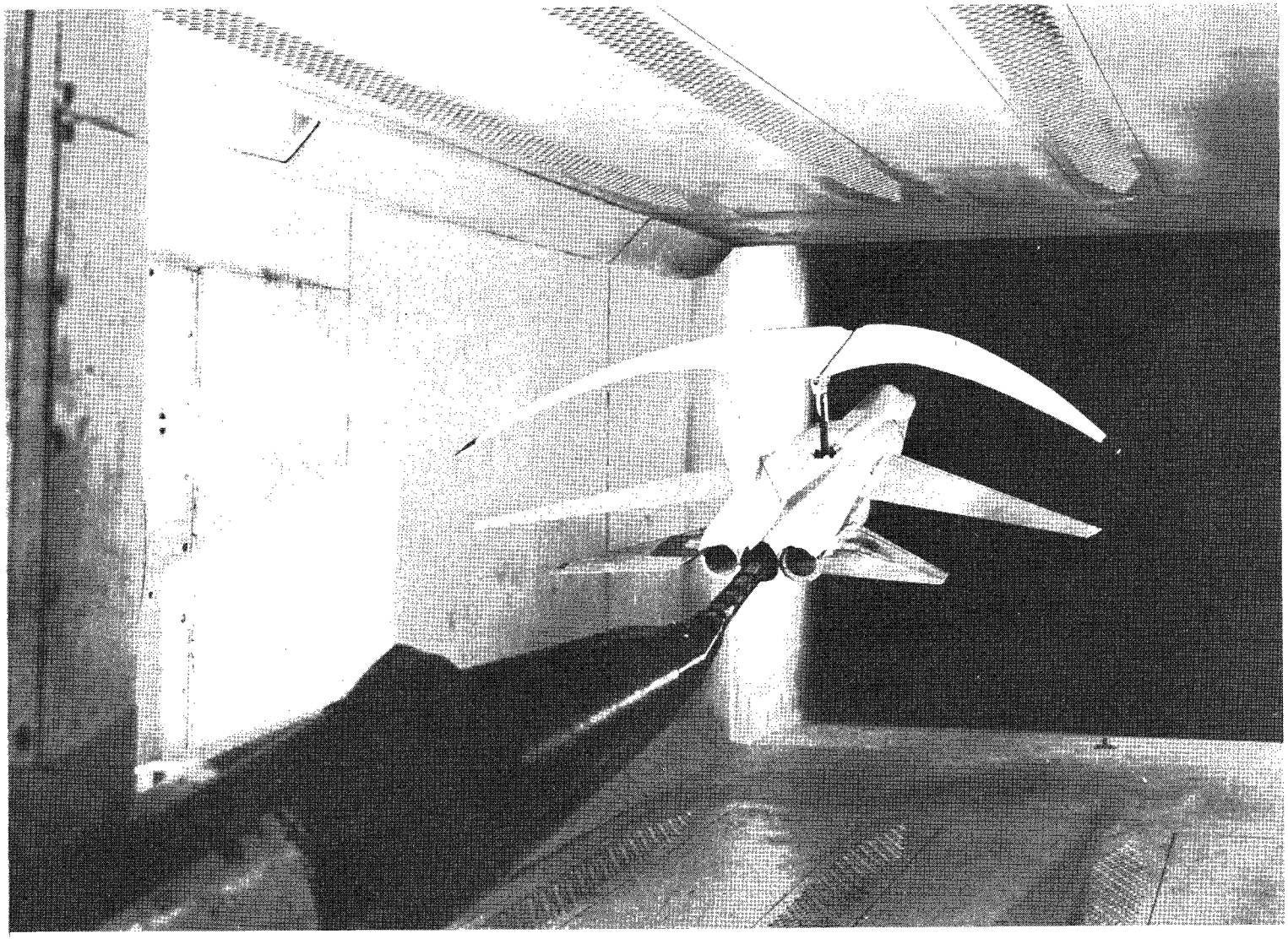

(b) Configuration $AP_1$. $h_p = 6.35$ in.; $l_p = -1.20$ in.; $i_p = 5°$. L-62-6763

Figure 2.- Continued.

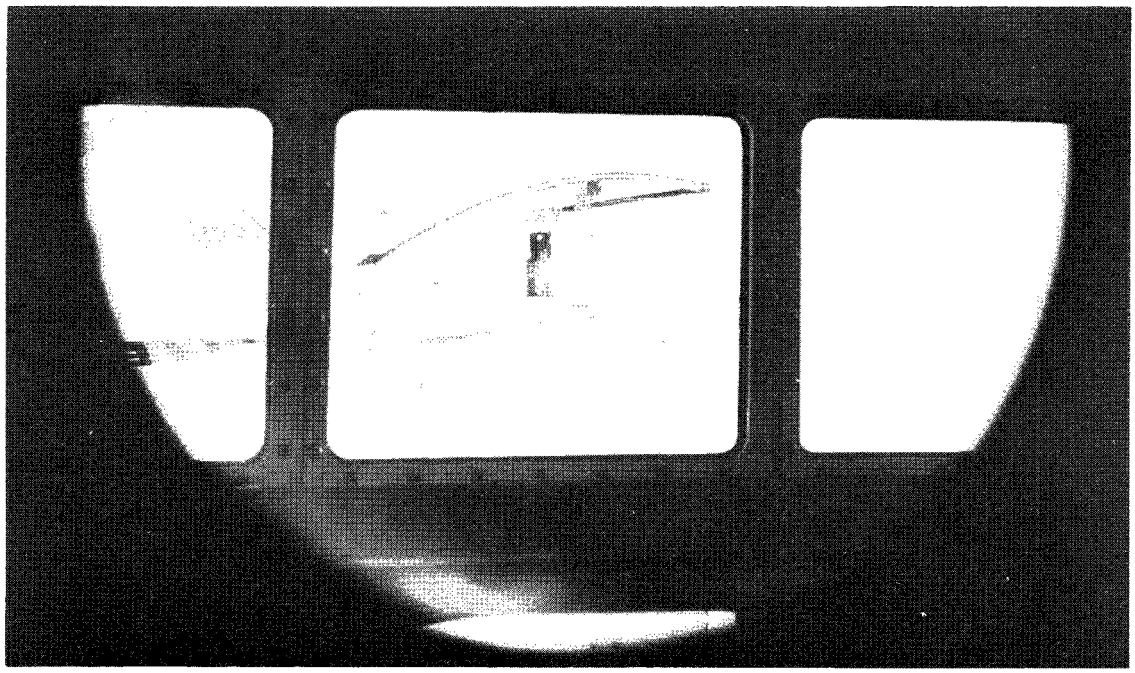

(b) Concluded. L-62-6765

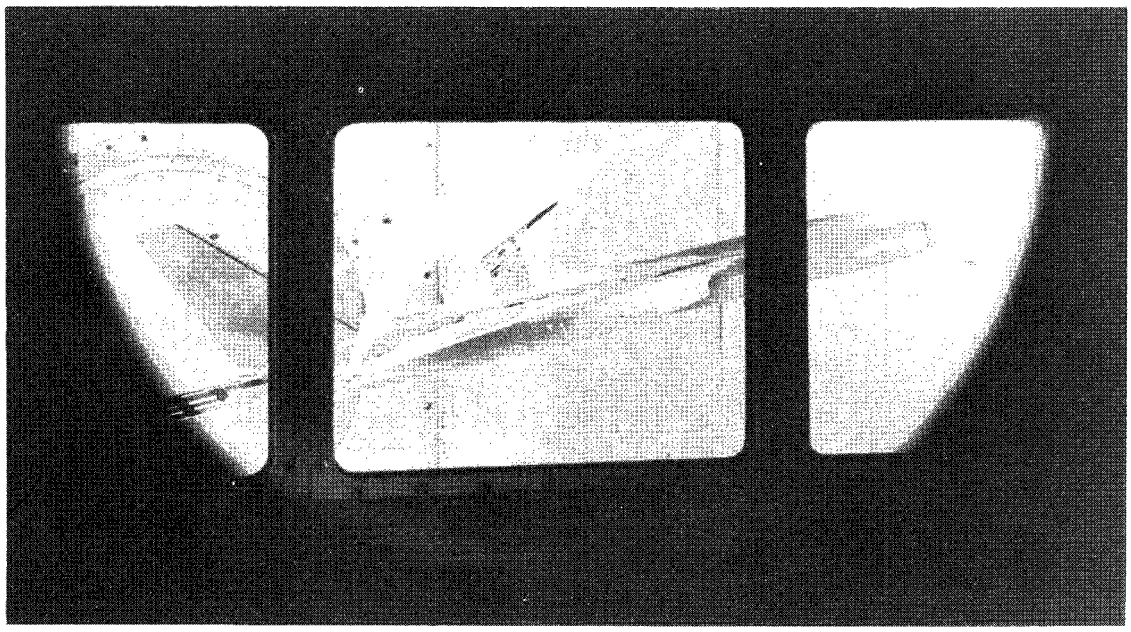

(c) Configuration $AP_4$. $h_p$ = 3.70 in.; $l_p$ = -1.20 in.; $i_p$ = 25°. L-62-6767

Figure 2.- Concluded.

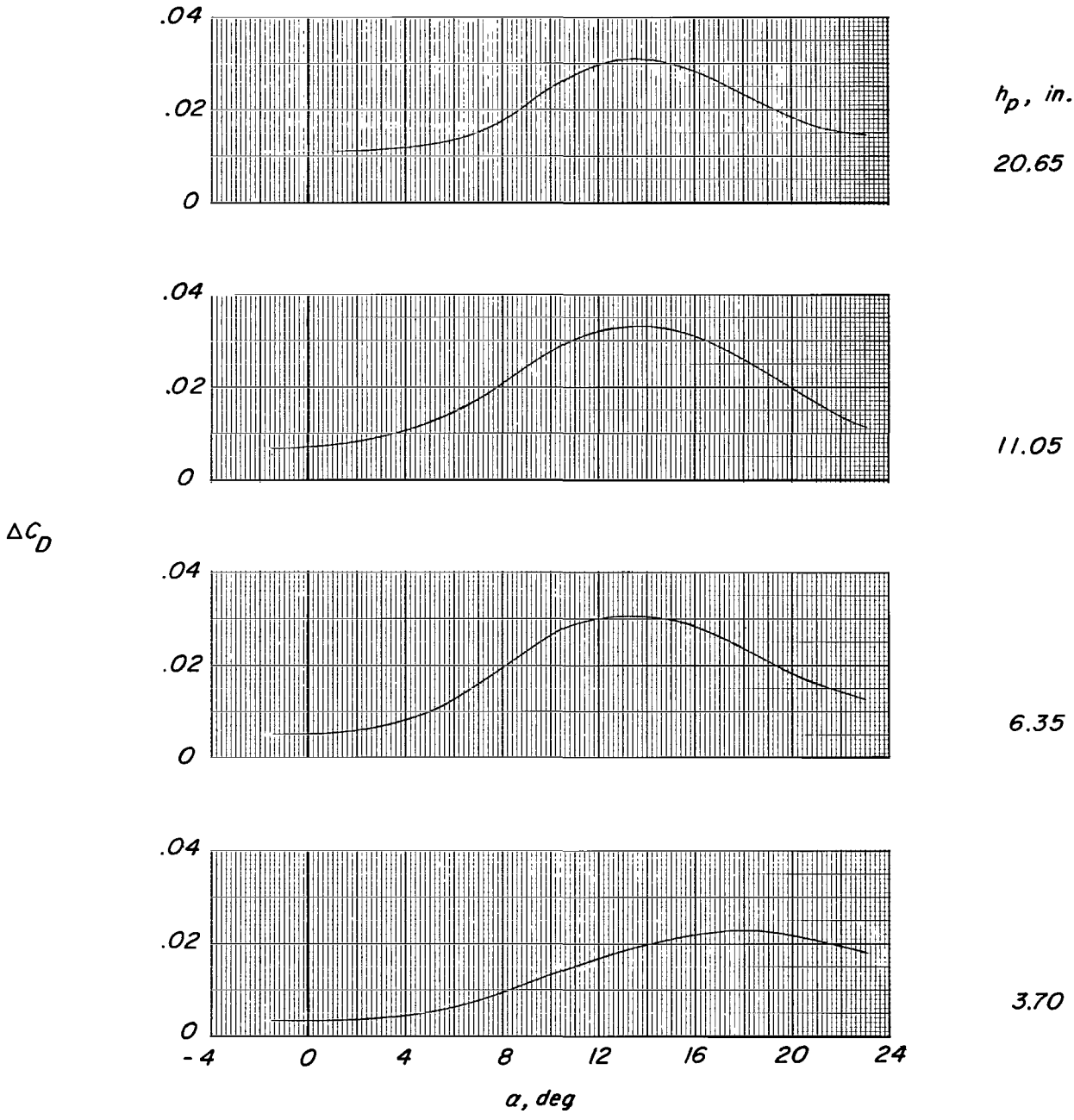


Figure 3.- Incremental drag due to the addition of the parawing support struts as a function of angle of attack. $l_p$ = -0.20 in.

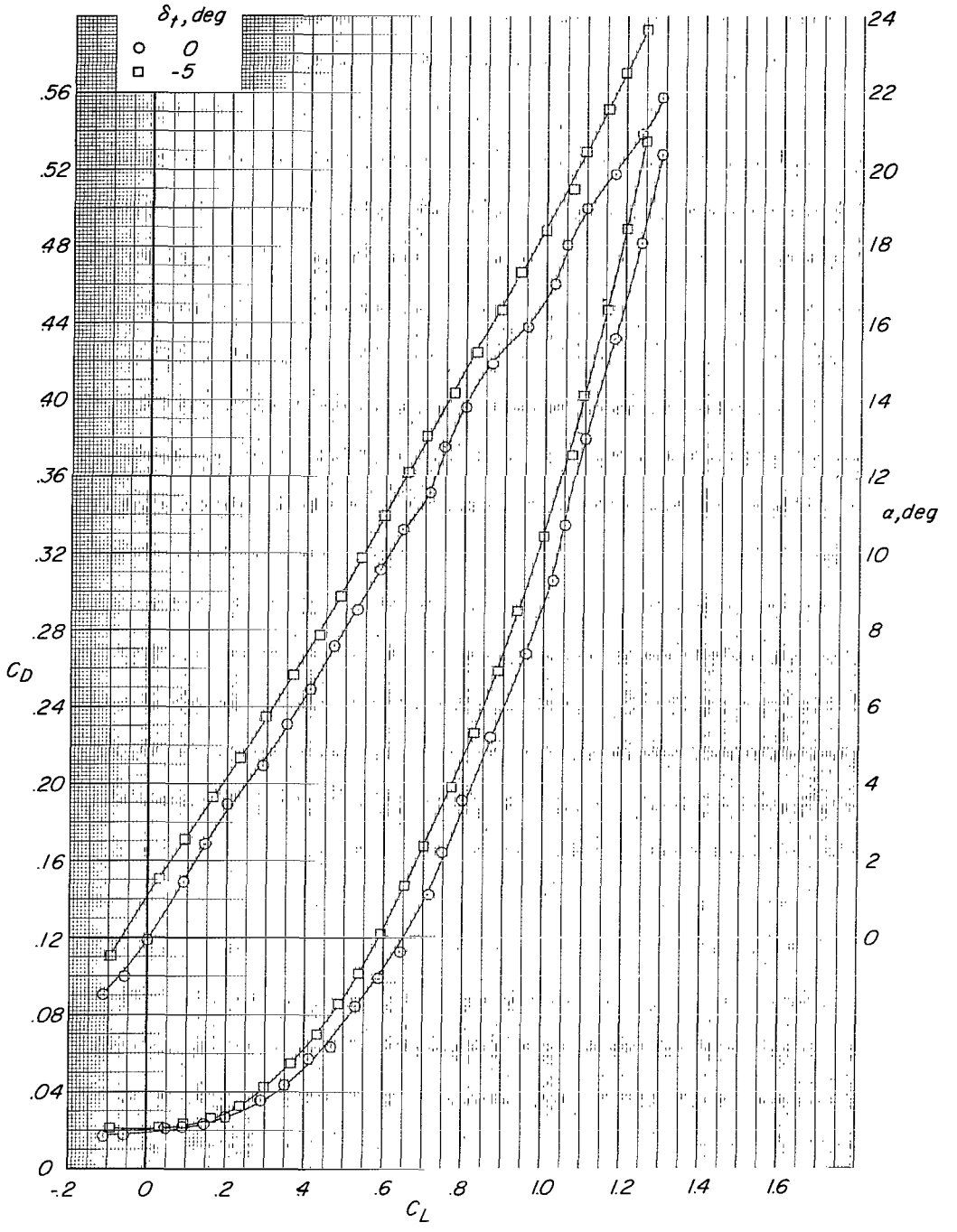


(a) Configuration A.

Figure 4.- Longitudinal aerodynamic characteristics for configurations A (airplane model alone) and $P_1$ (parawing alone).

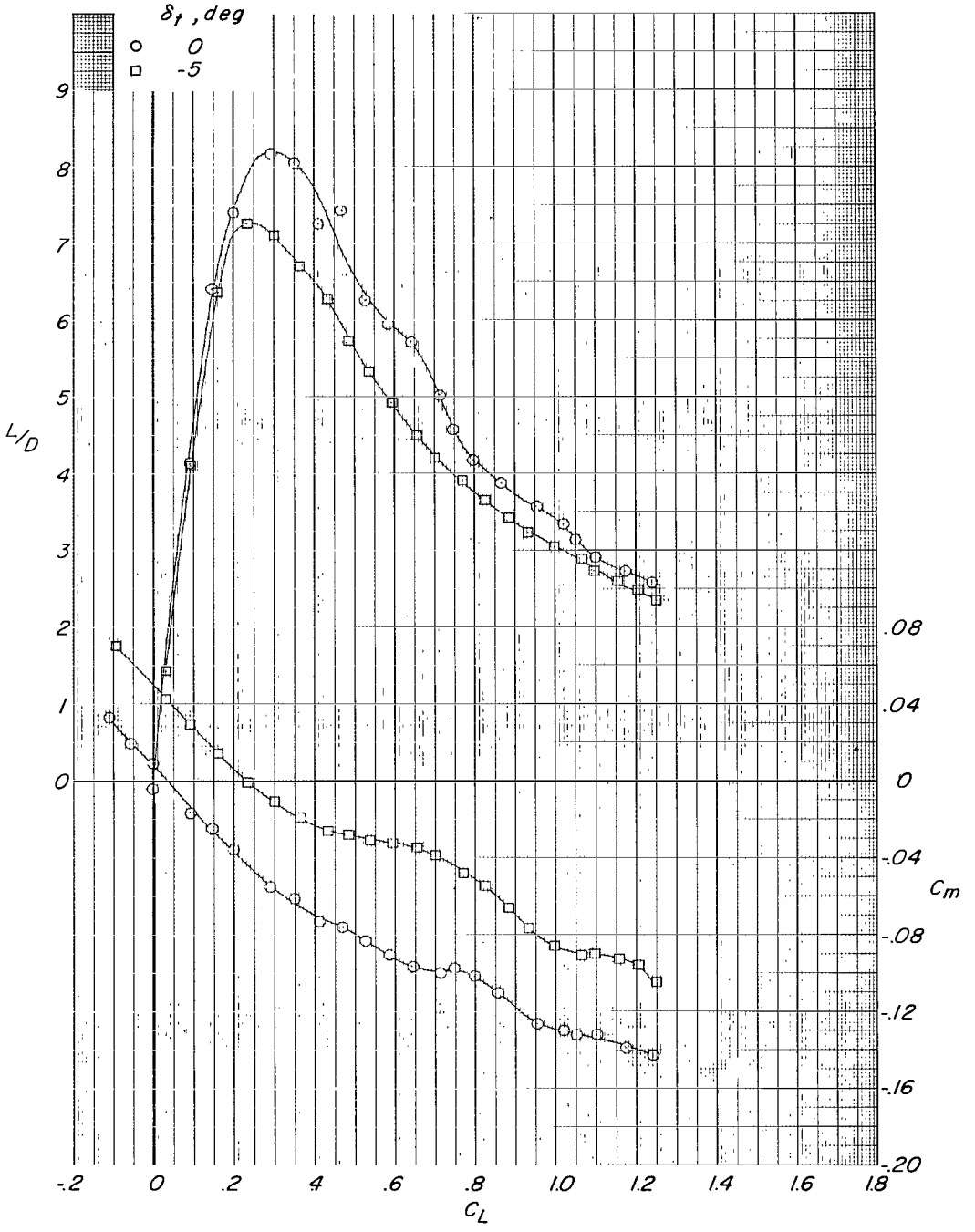


(a) Concluded.

Figure 4.- Continued.

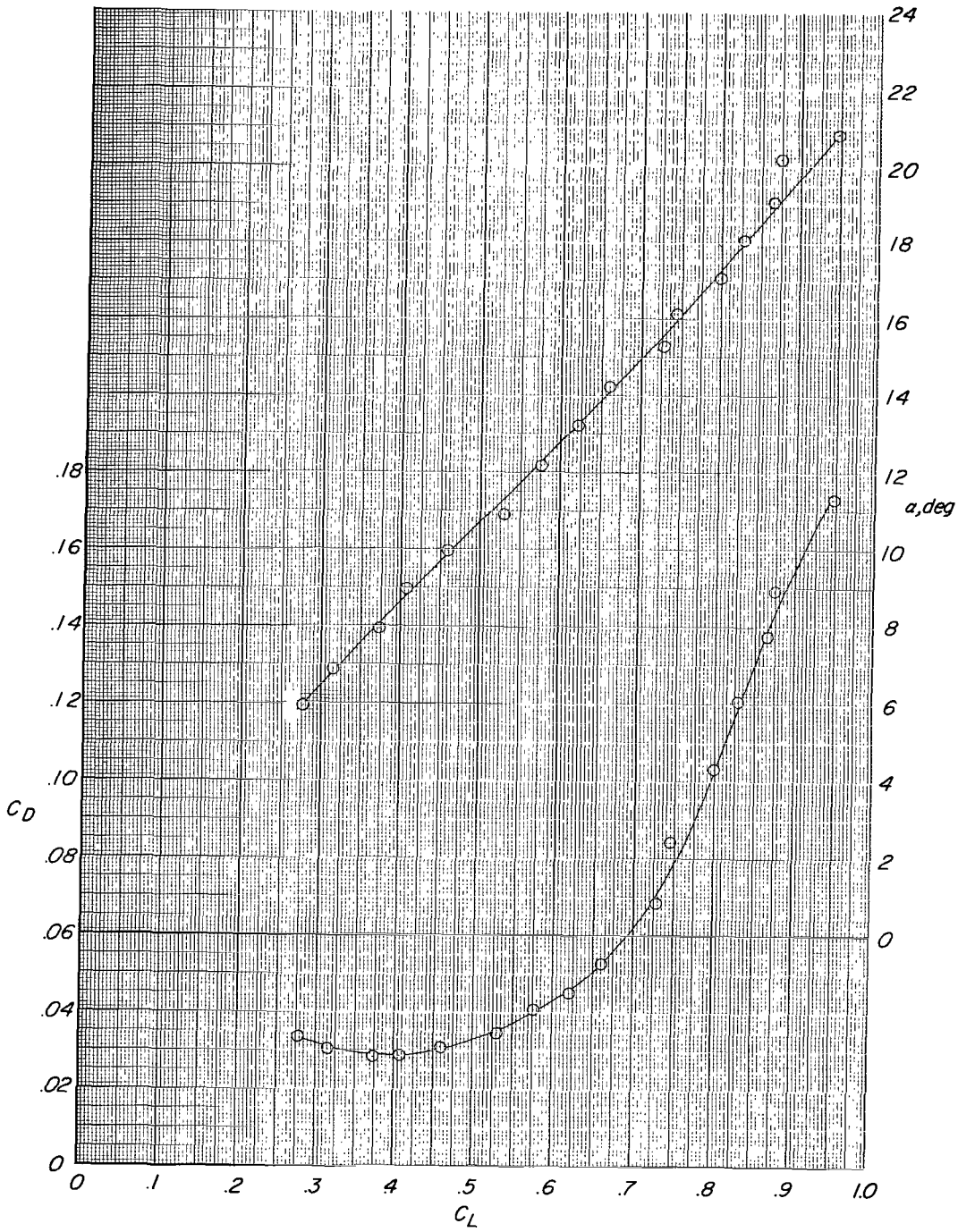


(b) Configuration $P_1$.

Figure 4.- Continued.

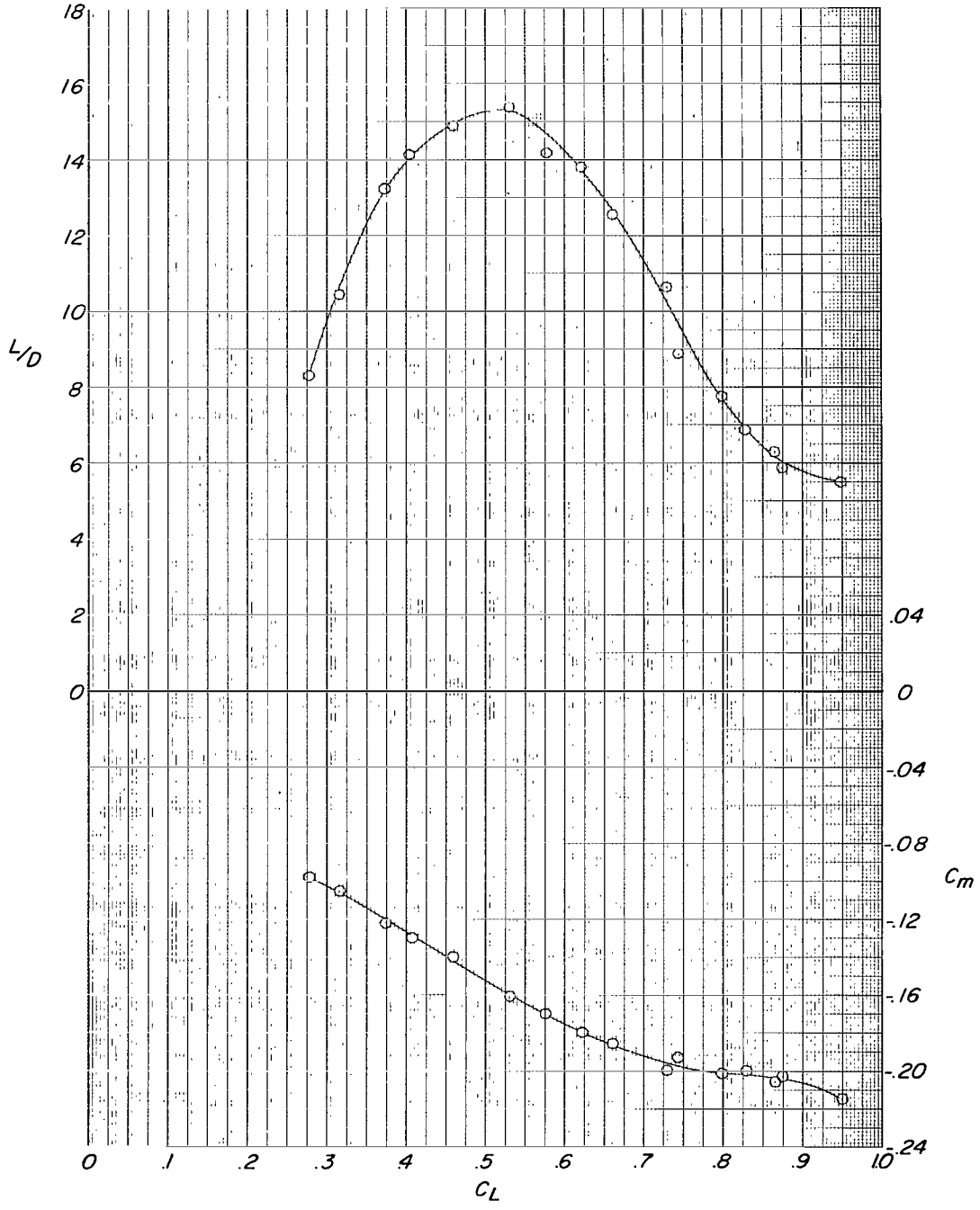


(b) Concluded.

Figure 4.- Concluded.

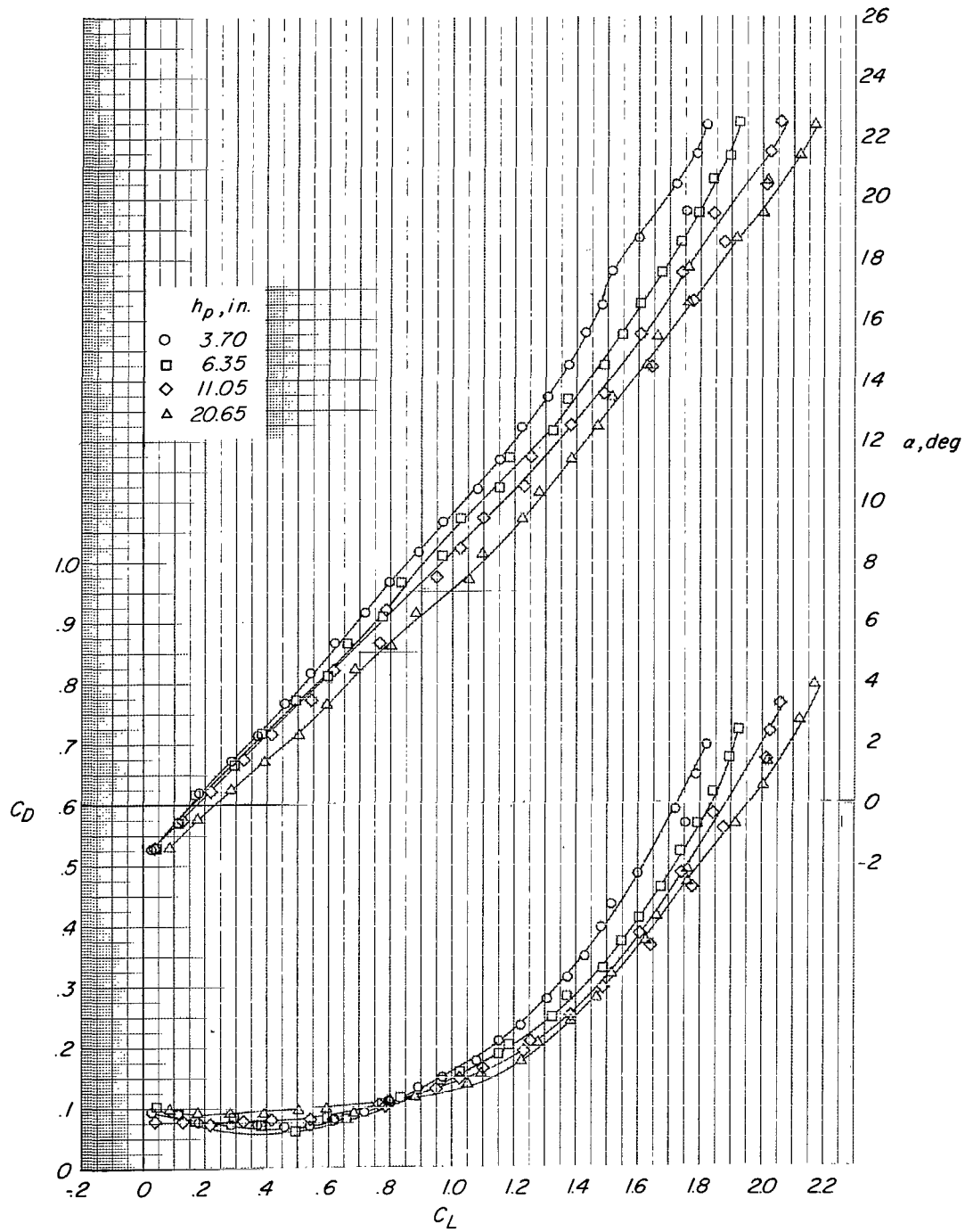


Figure 5.- Effect of vertical position of the parawing on the longitudinal aerodynamic characteristics for configuration $AP_1$. $l_p$ = -0.20 in.; $i_p = 5^\circ$; $\delta_t = 0^\circ$.

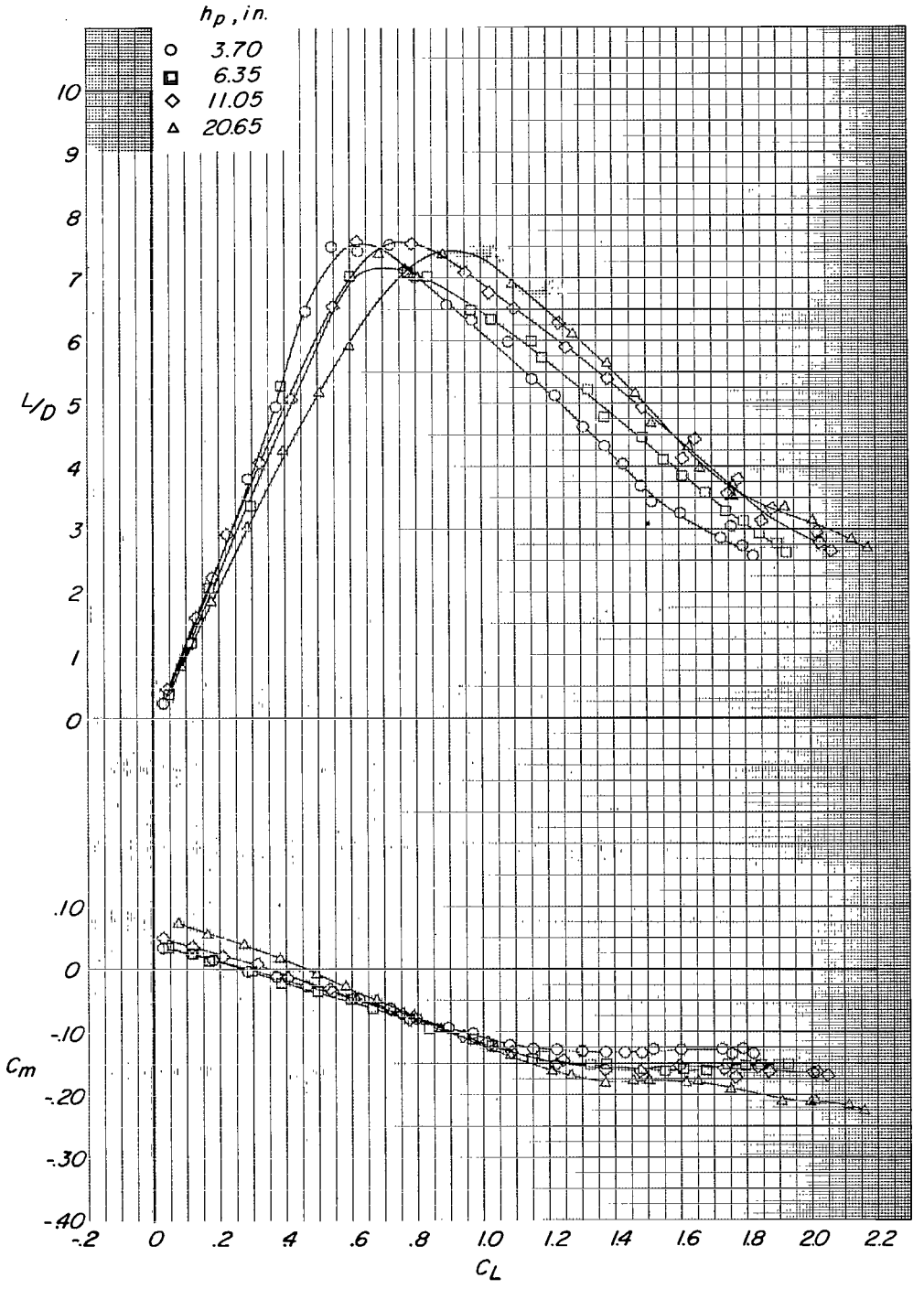


Figure 5.- Concluded.

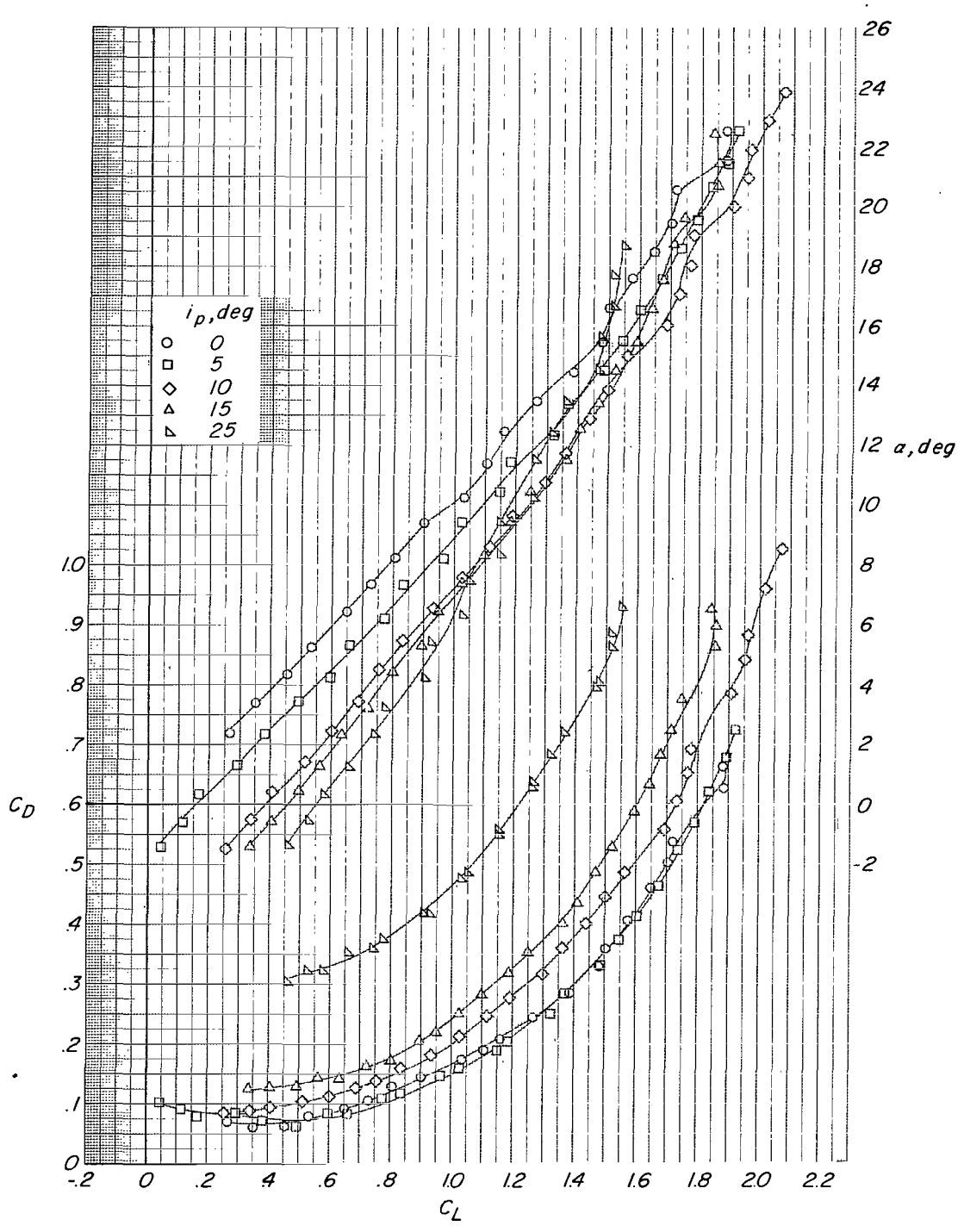


Figure 6.- Effect of parawing keel angle on the longitudinal aerodynamic characteristics for configuration $AP_1$. $h_p$ = 6.35 in.; $l_p$ = -0.20 in.; $\delta_t$ = 0°.

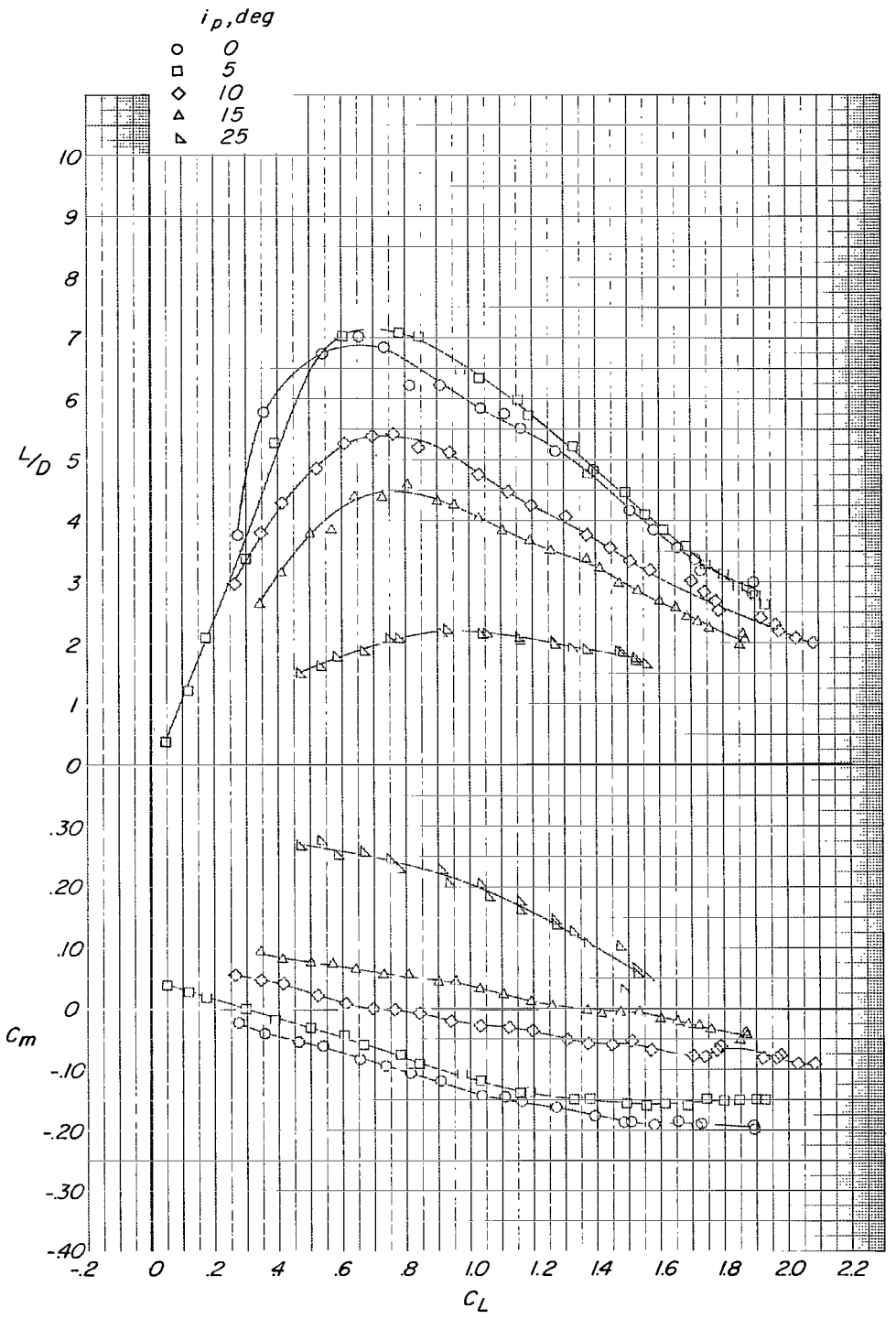


Figure 6.- Concluded.

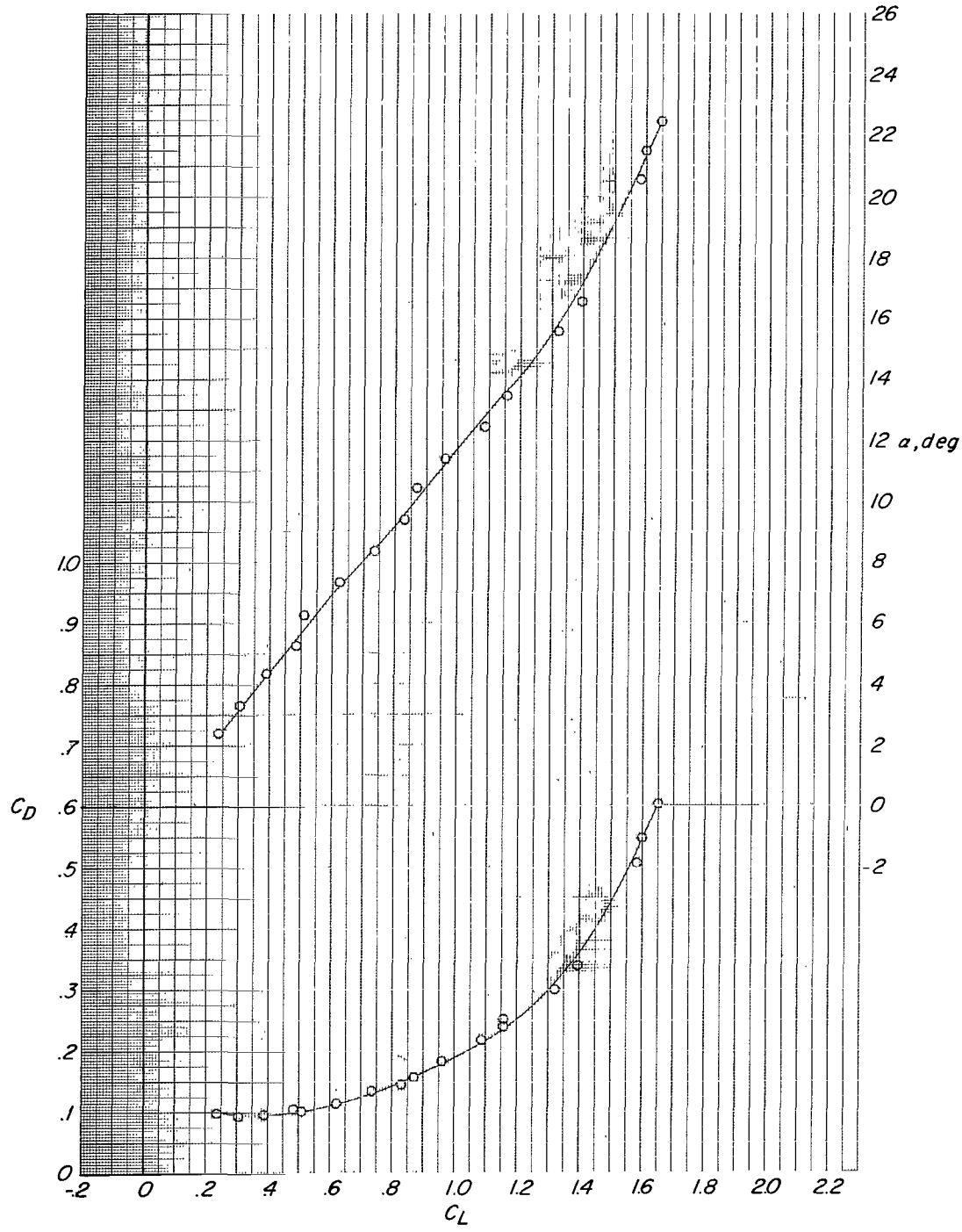


Figure 7.- Longitudinal aerodynamic characteristics for configuration $AP_1$. $h_p$ = 1.38 in.; $l_p$ = -0.20 in.; $i_p$ = 0°; $\delta_t$ = 0°.

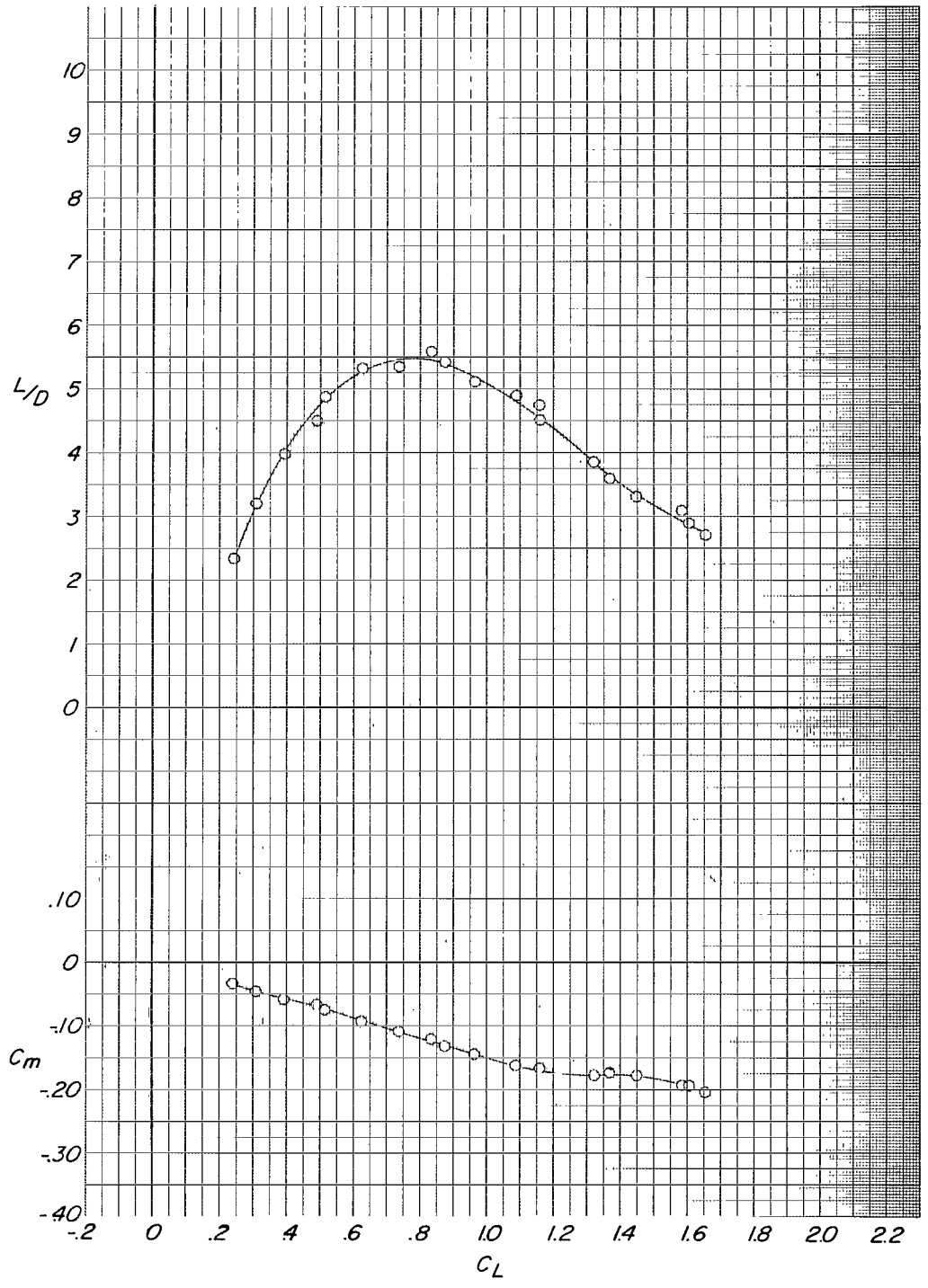


Figure 7.- Concluded.

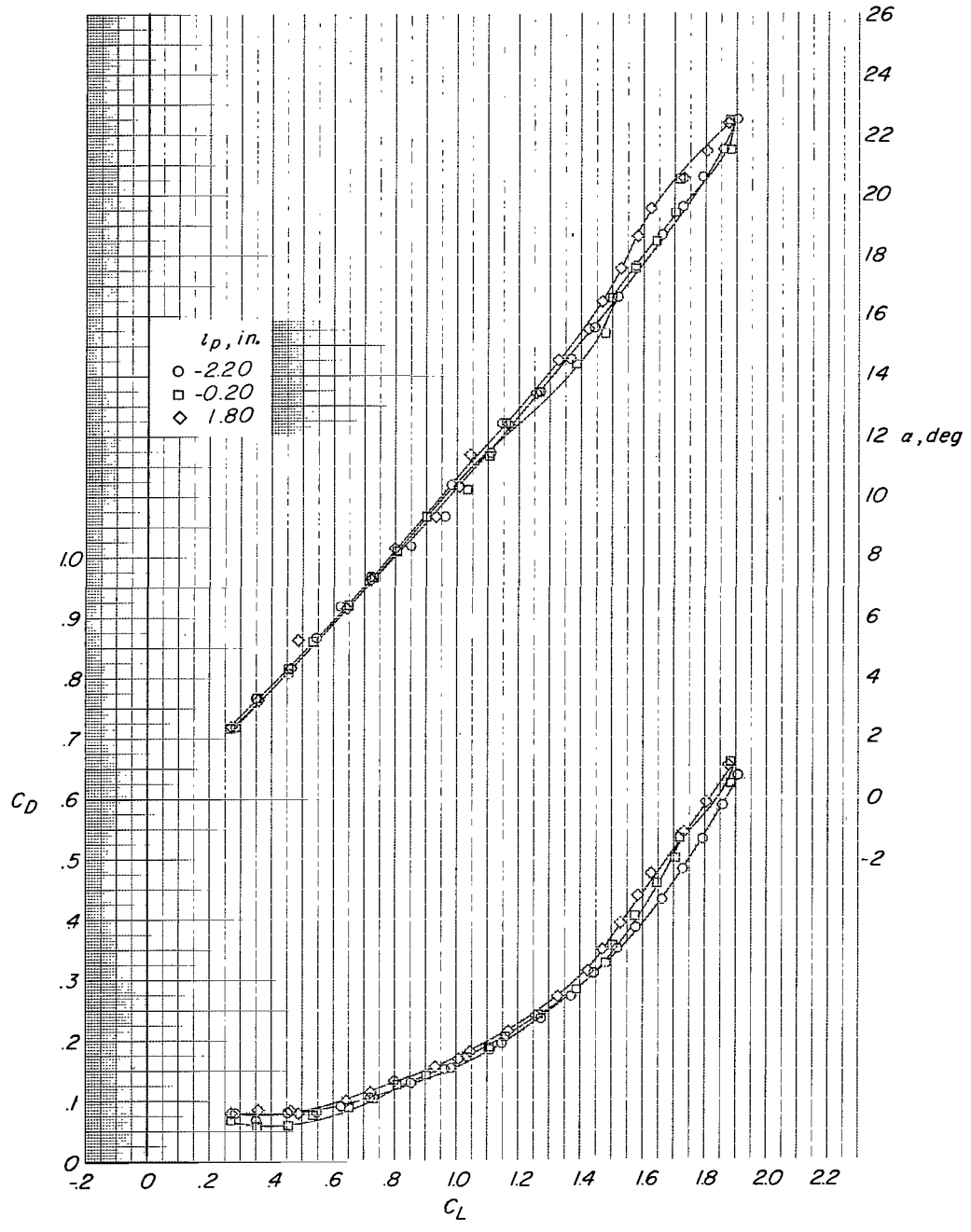


(a) $h_p$ = 6.35 in.

Figure 8.- Effect of locating the parawing pivot axis fore and aft of the airplane center of gravity on the longitudinal aerodynamic characteristics for configuration $AP_1$. $i_p = 0^\circ$; $\delta_t = 0^\circ$.

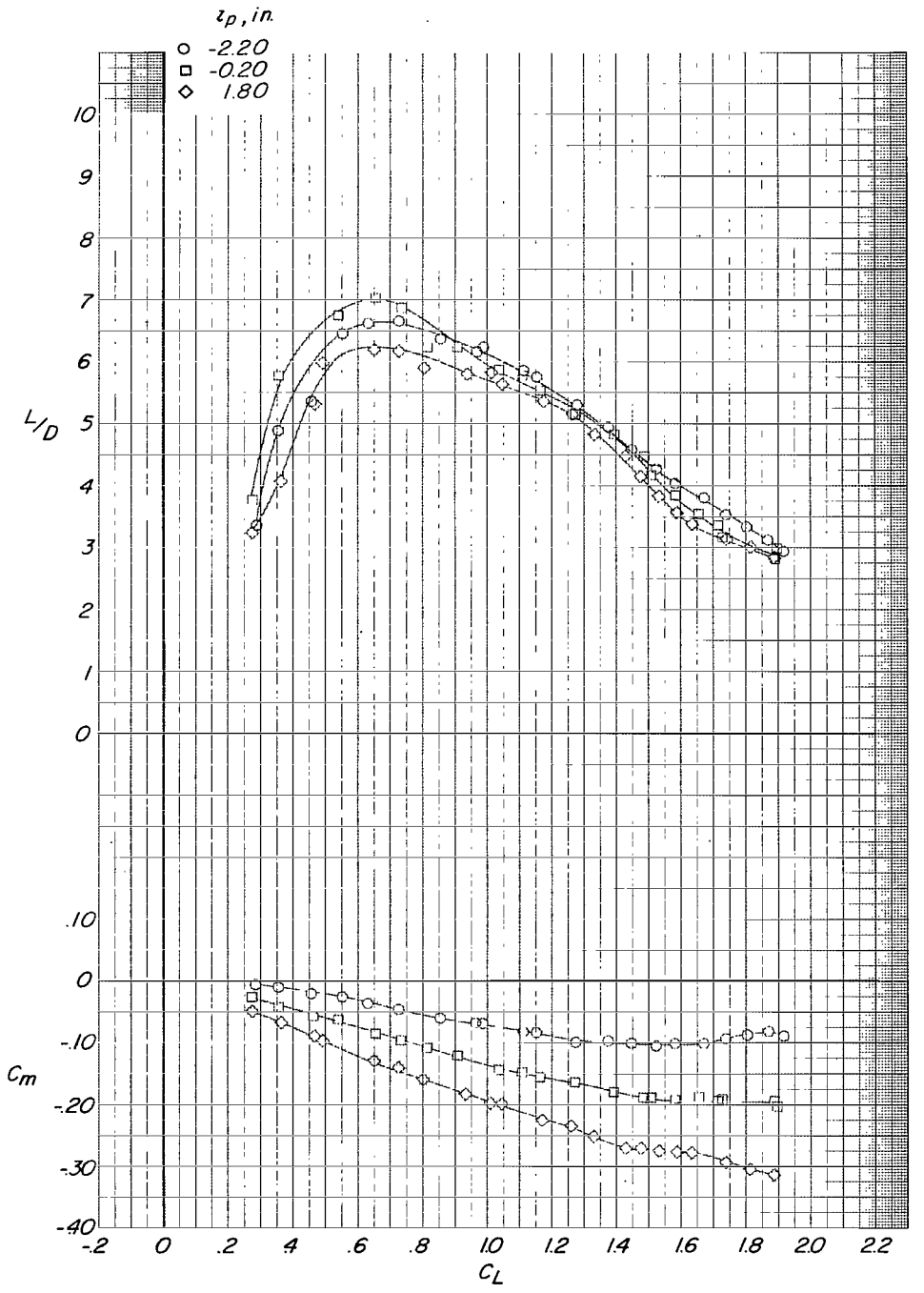


(a) Concluded.

Figure 8.- Continued.

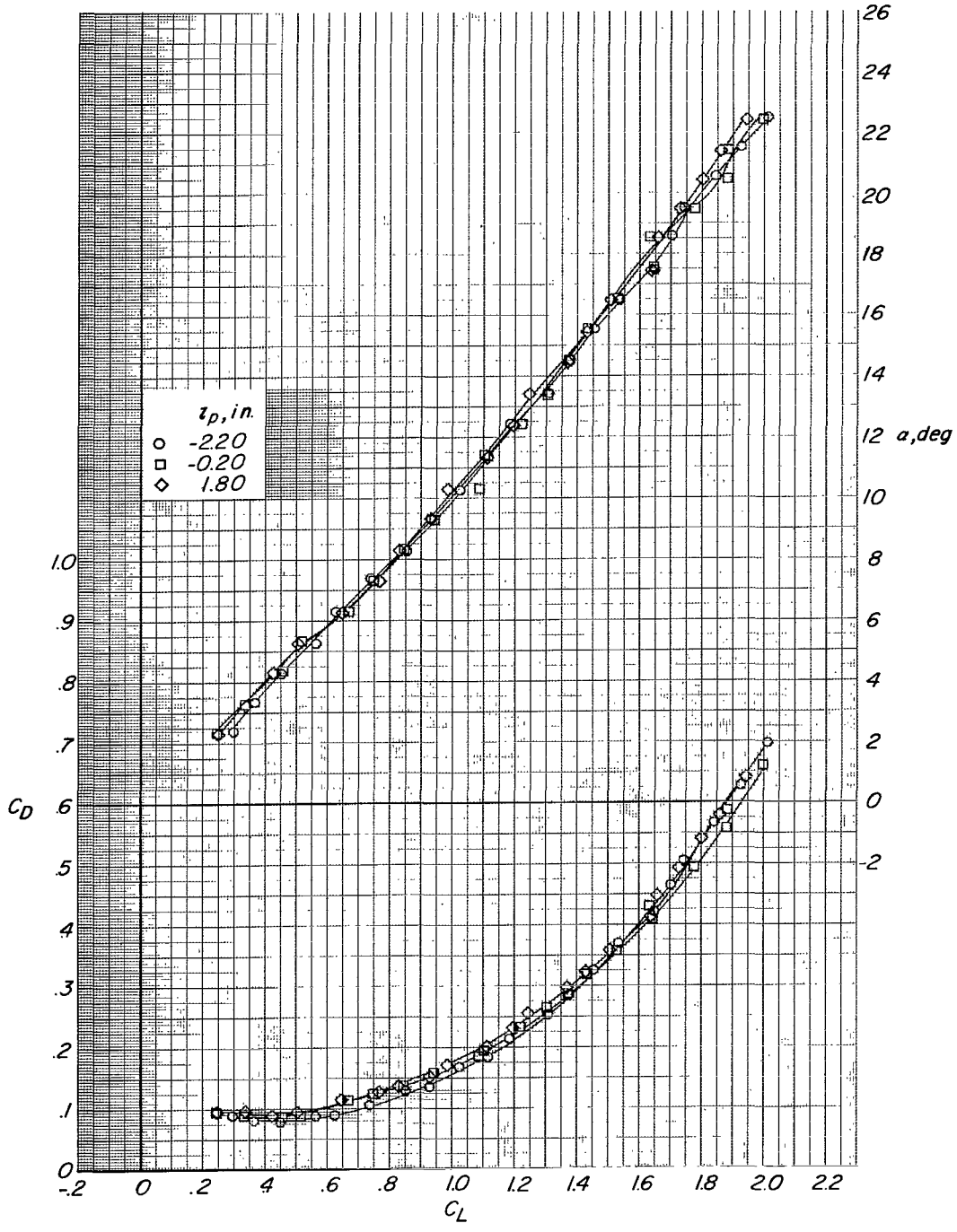


(b) $h_p$ = 11.05 in.

Figure 8.- Continued.

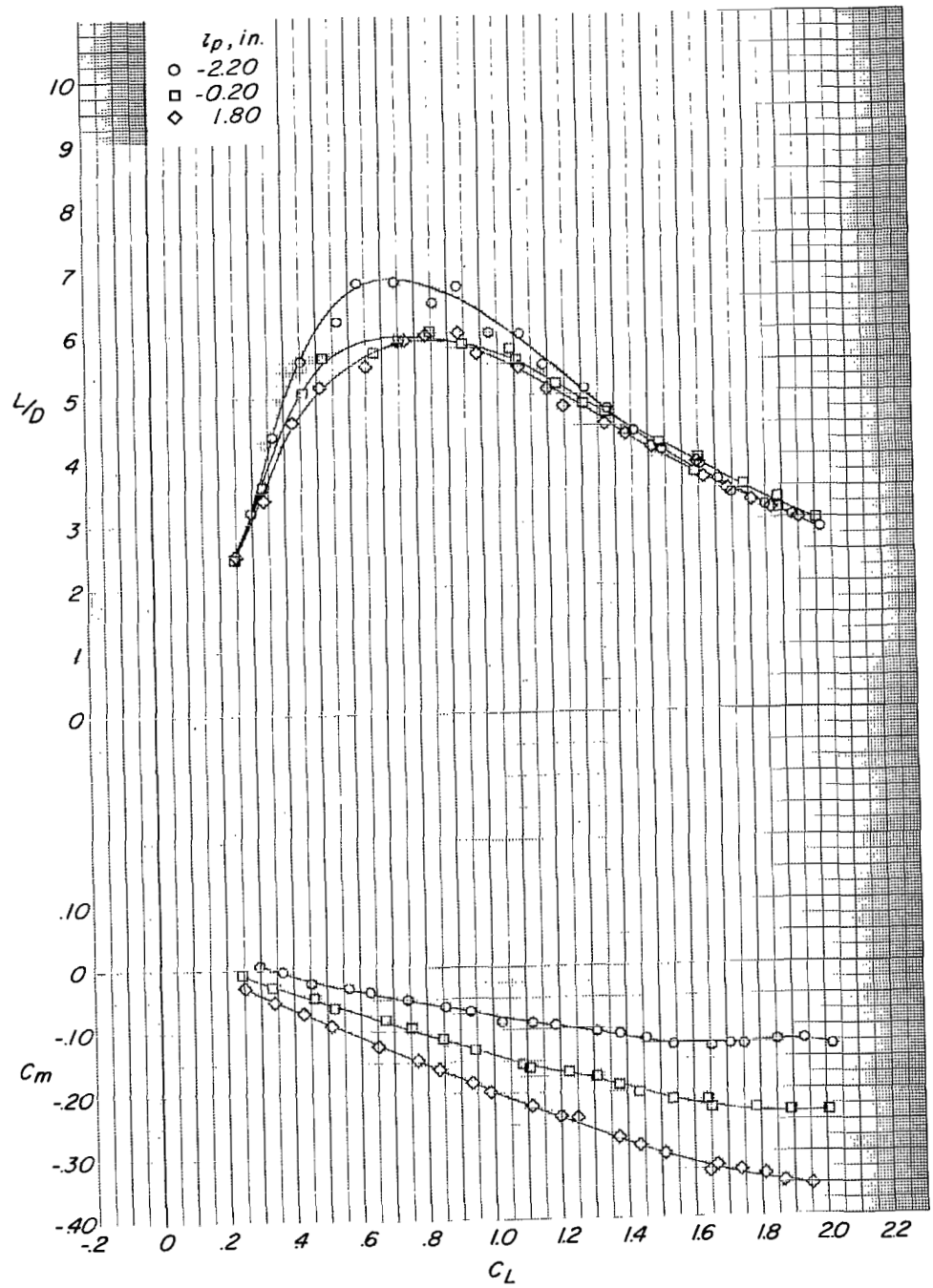


(b) Concluded.

Figure 8.- Concluded.

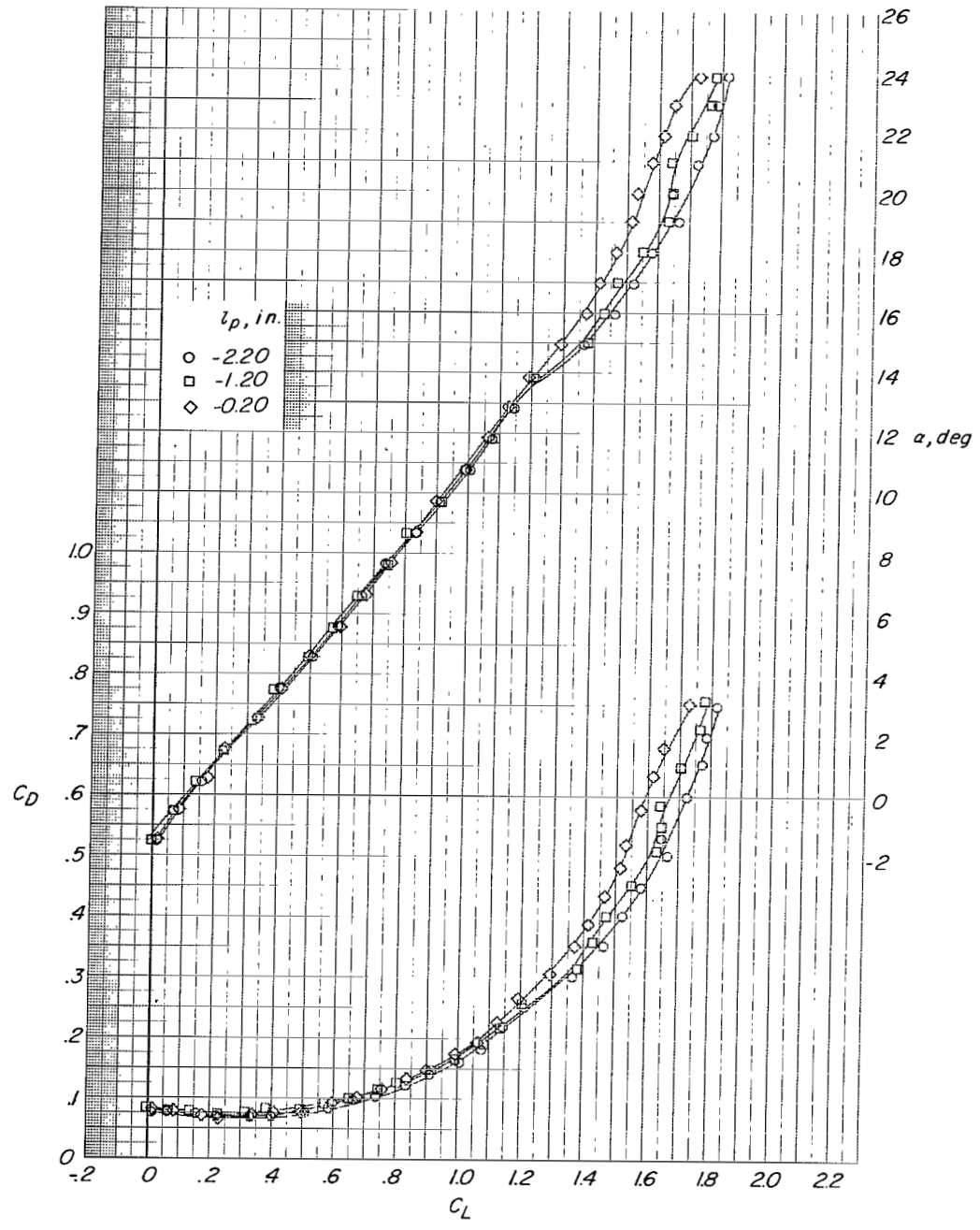


(a) $h_p$ = 1.38 in.

Figure 9.- Effect of locating the parawing pivot axis fore and aft of the airplane center of gravity on the longitudinal aerodynamic characteristics for configuration $AP_1$. $i_p = 5^\circ$; $\delta_t = 0^\circ$.

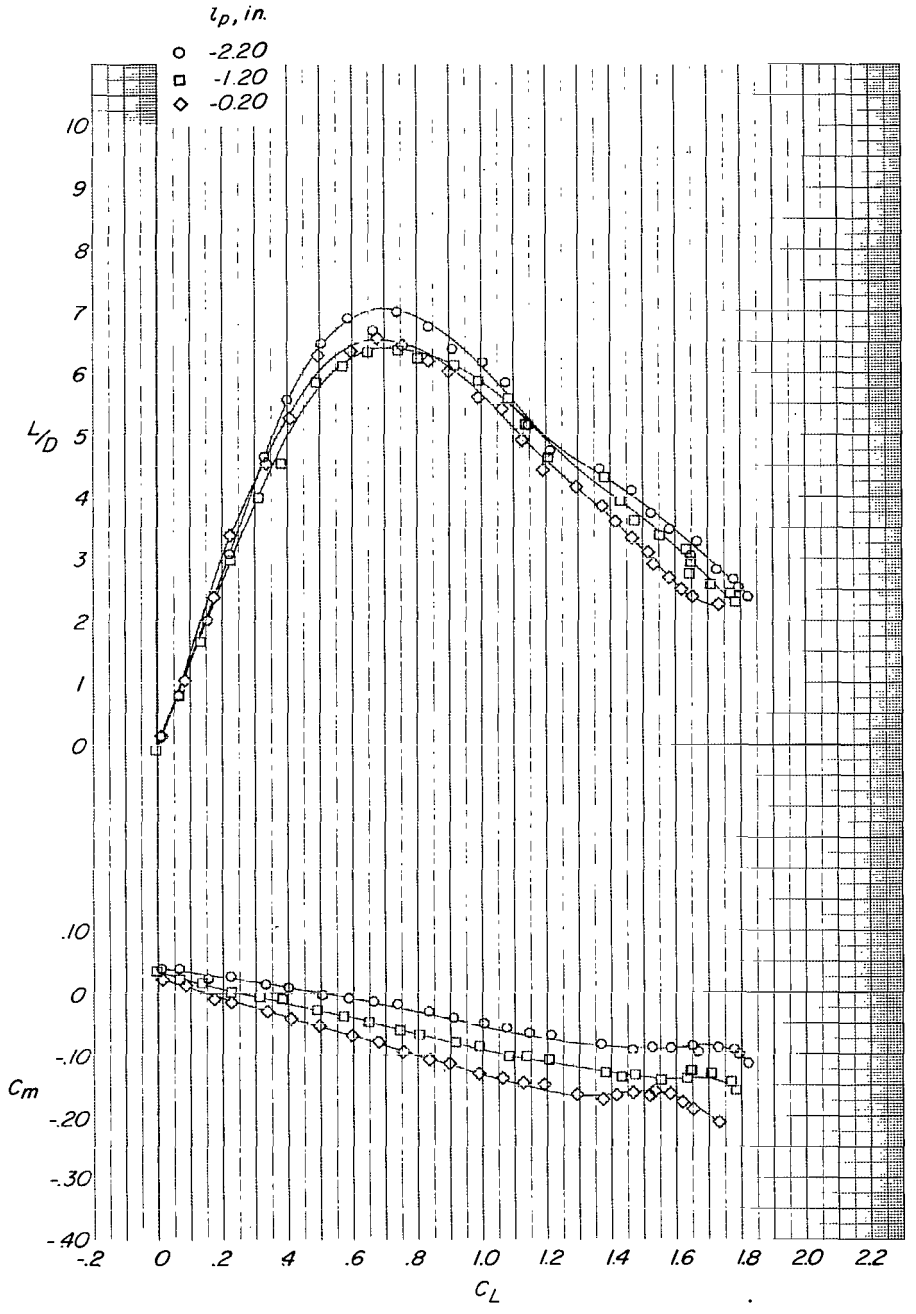


(a) Concluded.

Figure 9.- Continued.

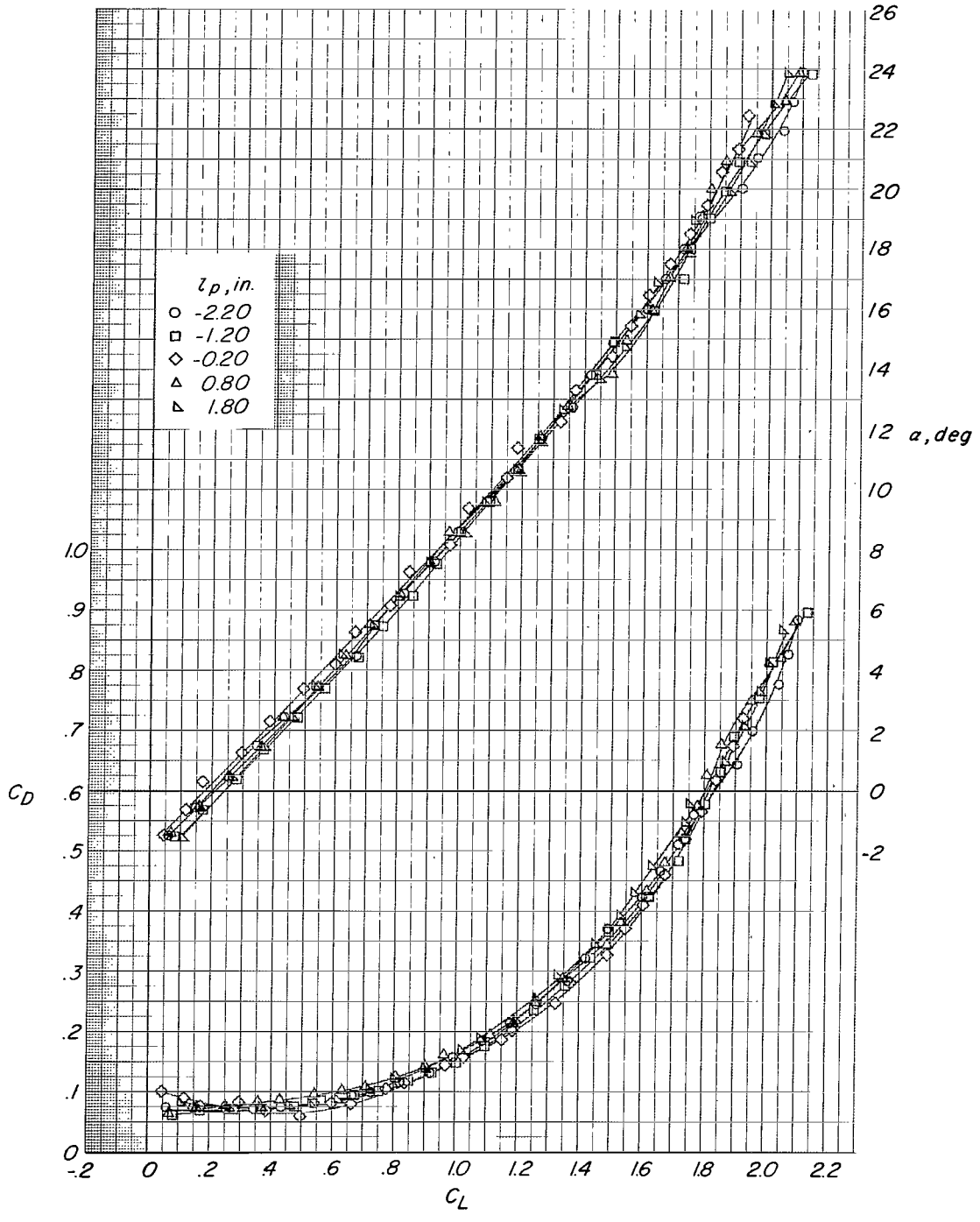


(b) $h_p$ = 6.35 in.

Figure 9.- Continued.

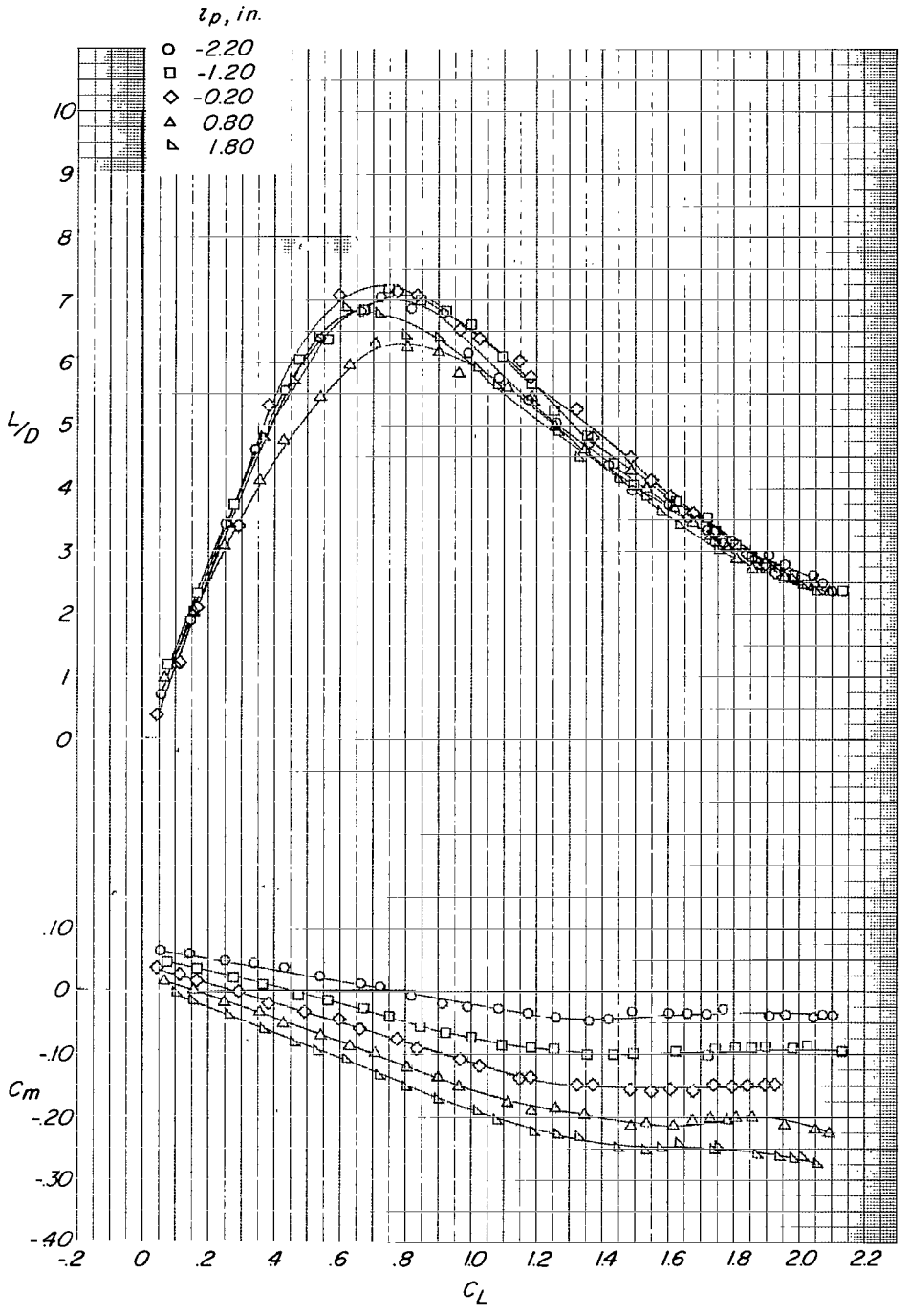


(b) Concluded.

Figure 9.- Continued.

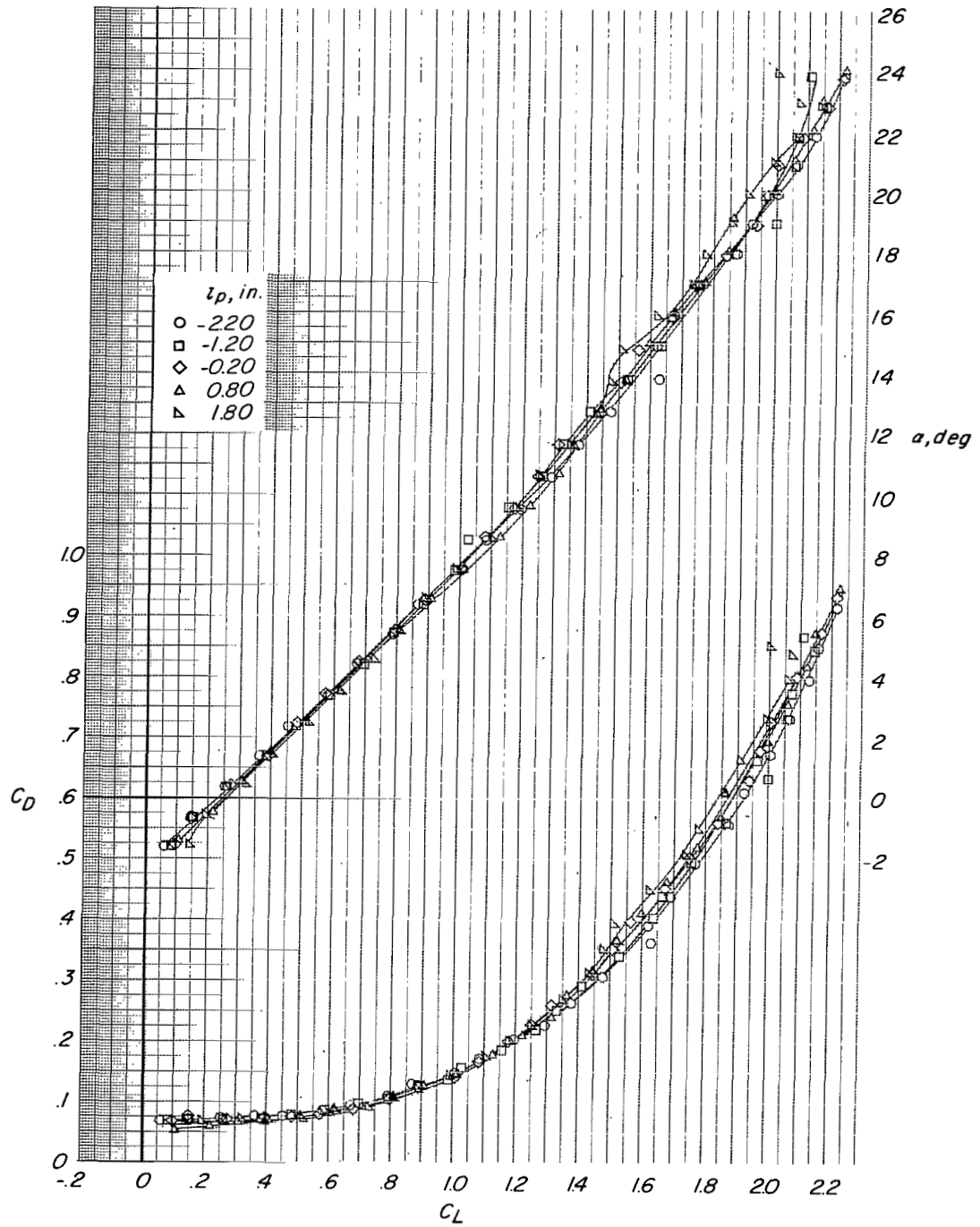


(c) $h_p$ = 11.05 in.

Figure 9.- Continued.

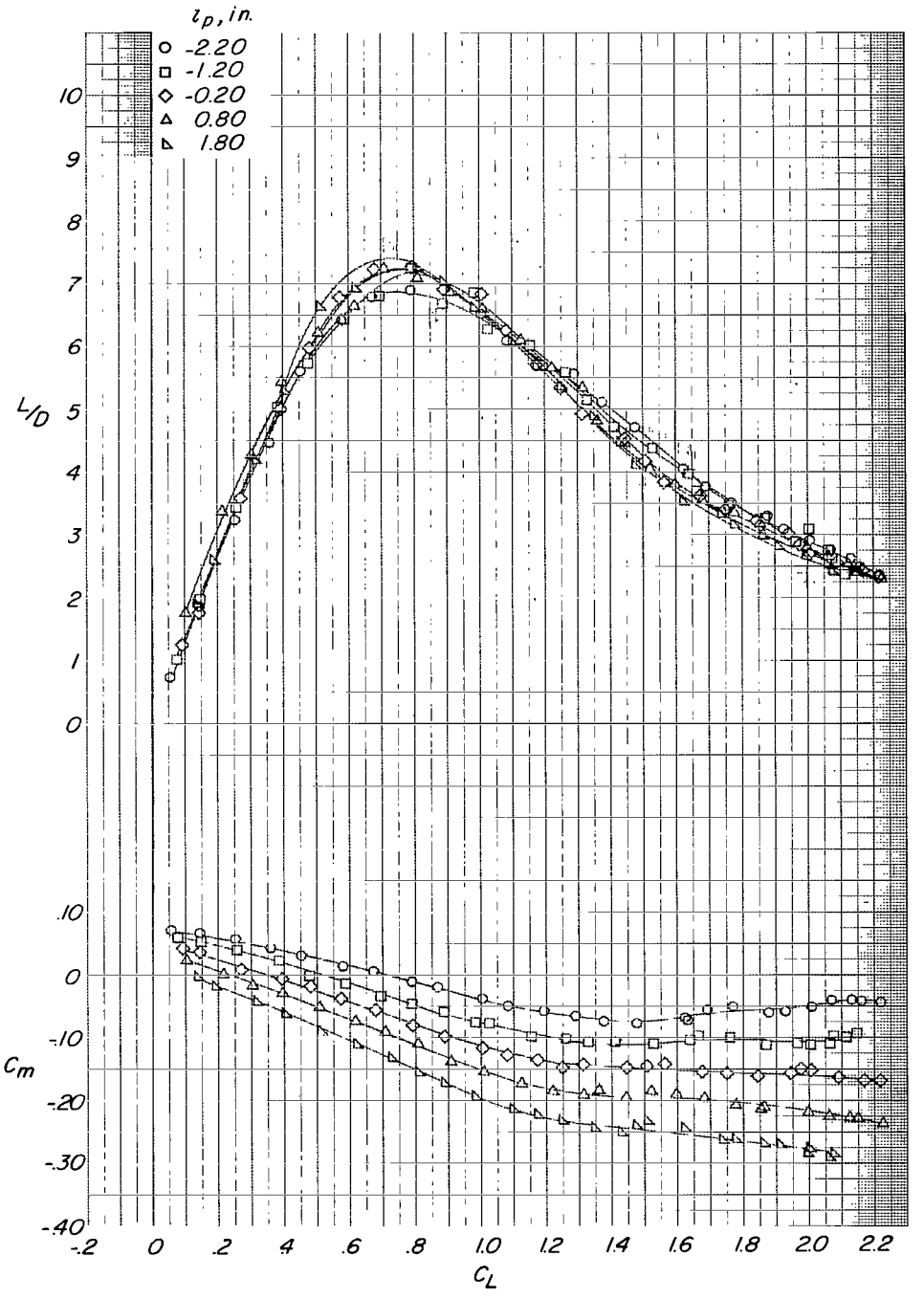


(c) Concluded.

Figure 9.- Concluded.

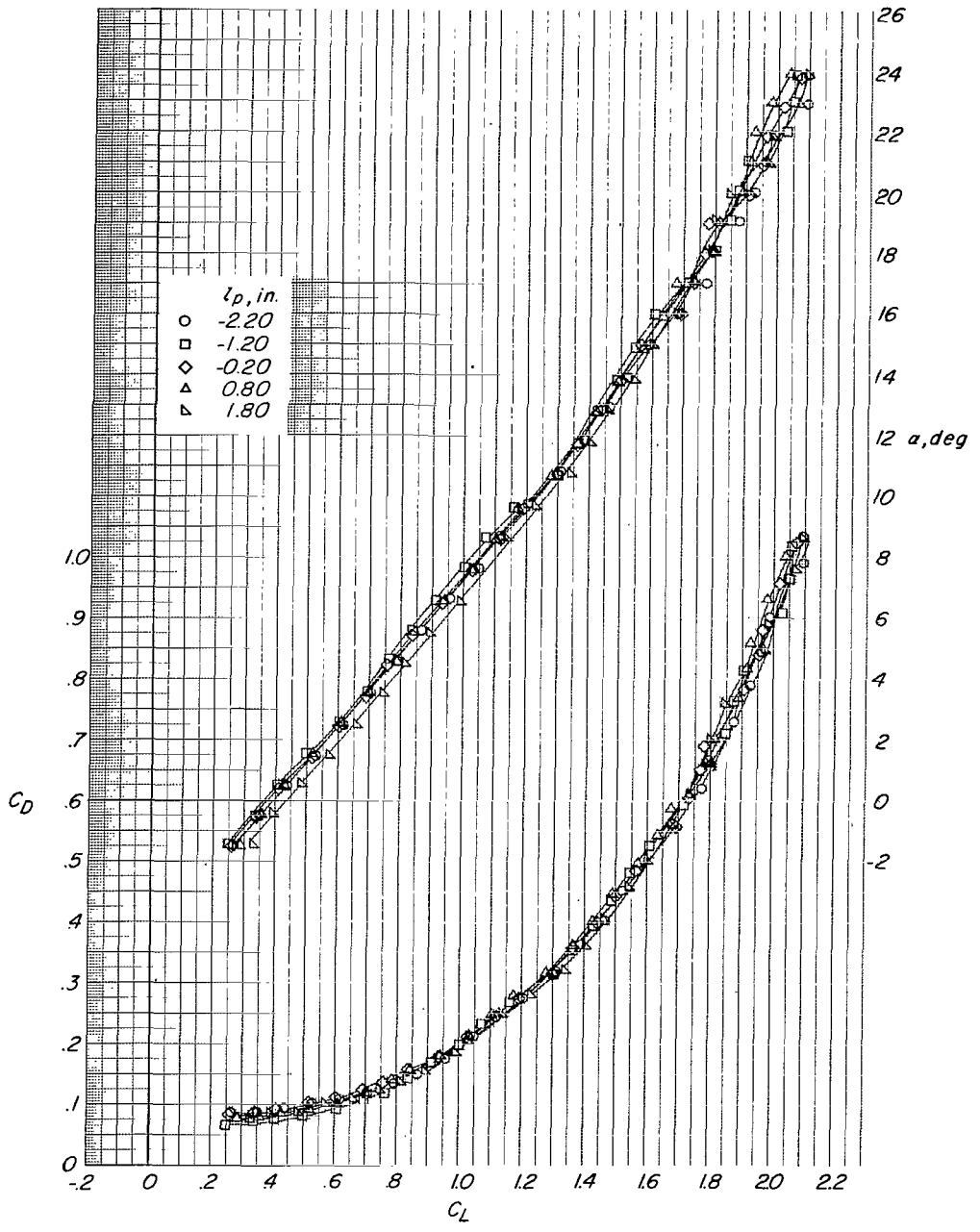


(a) $h_p$ = 6.35 in.

Figure 10.- Effect of locating the parawing pivot axis fore and aft of the airplane center of gravity on the longitudinal aerodynamic characteristics for configuration $AP_1$. $i_p = 10^o$; $\delta_t = 0^o$.

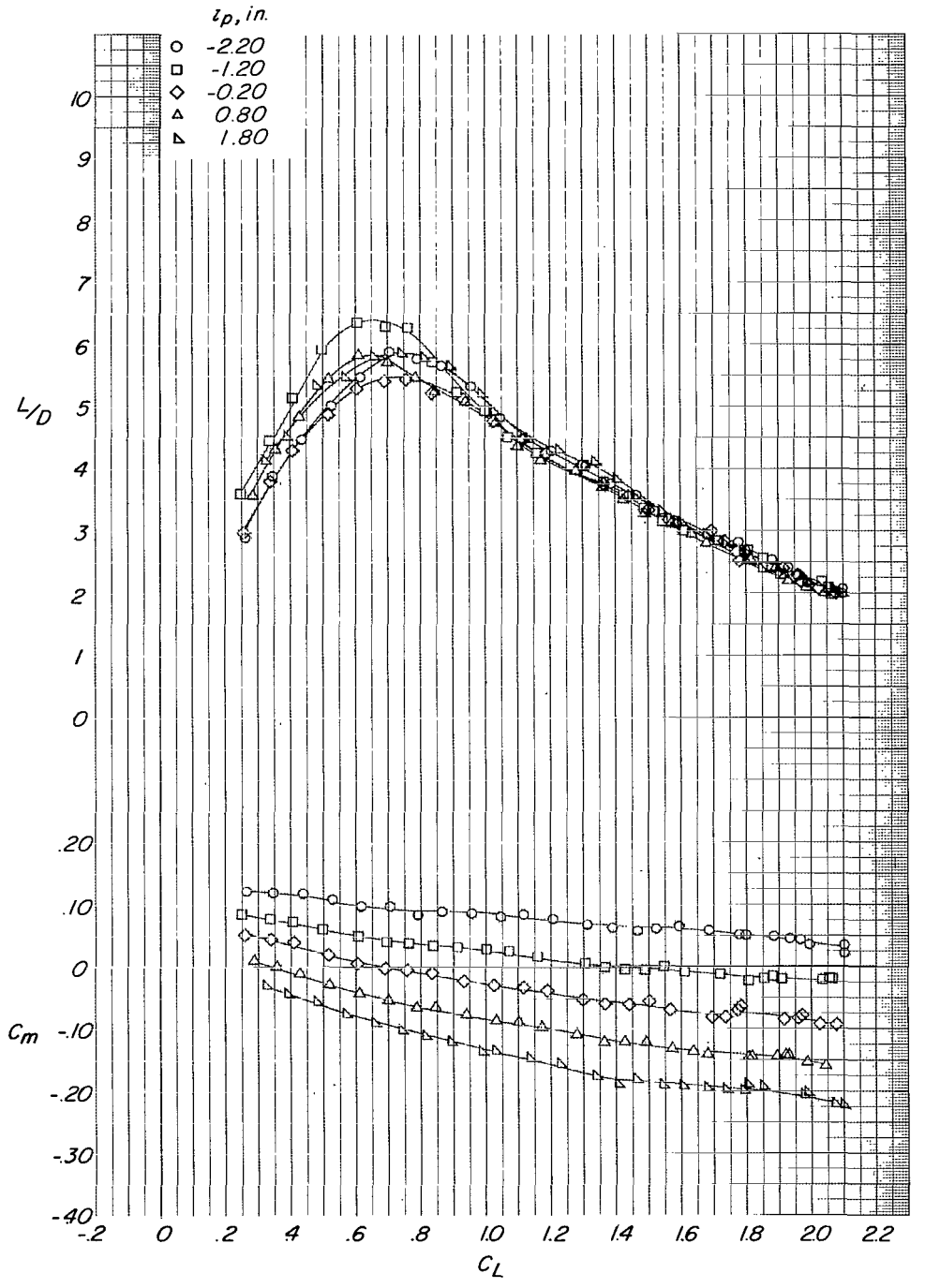


(a) Concluded.

Figure 10.- Continued.

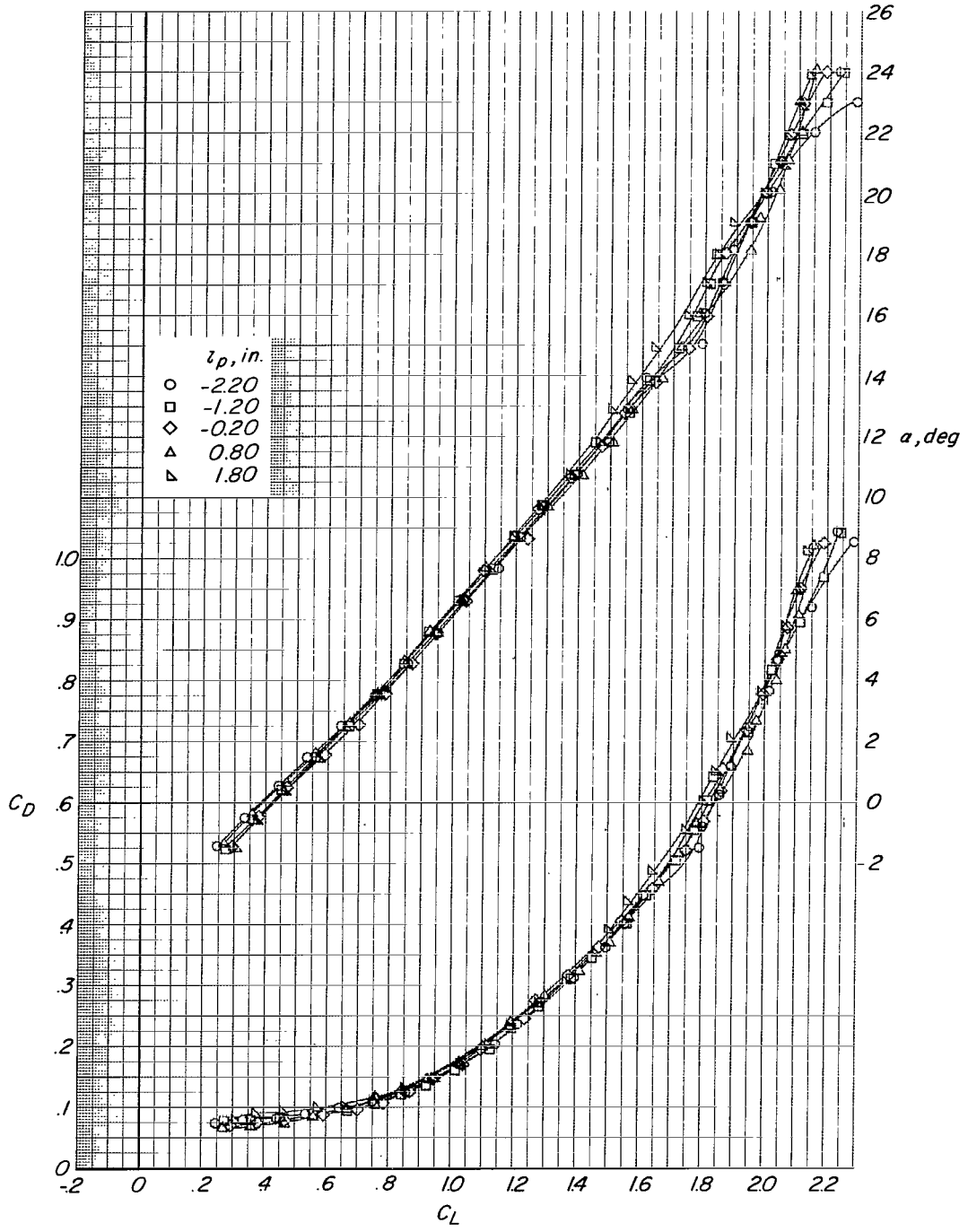


(b) $h_p$ = 11.05 in.

Figure 10.- Continued.

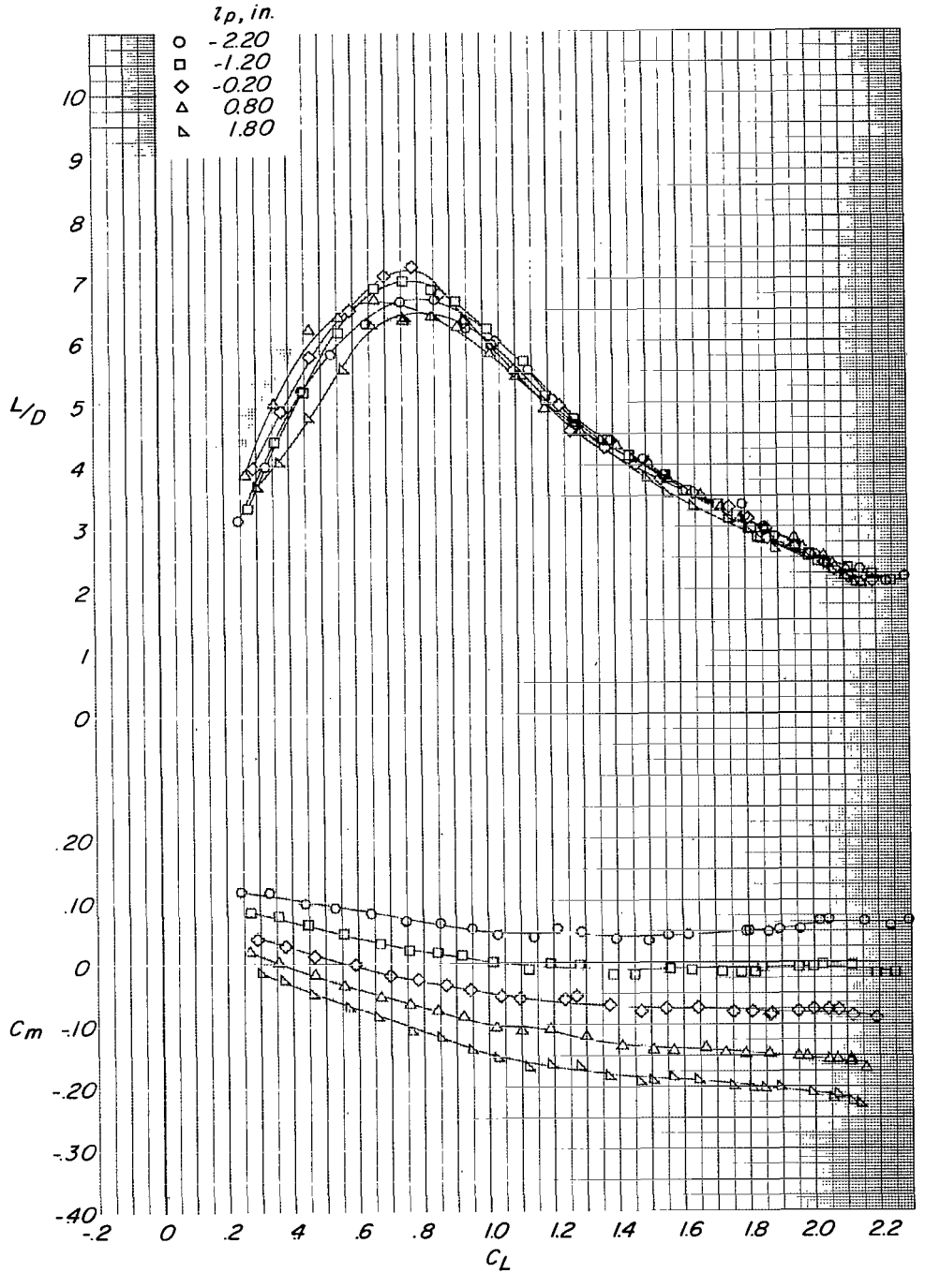


(b) Concluded.

Figure 10.- Concluded.

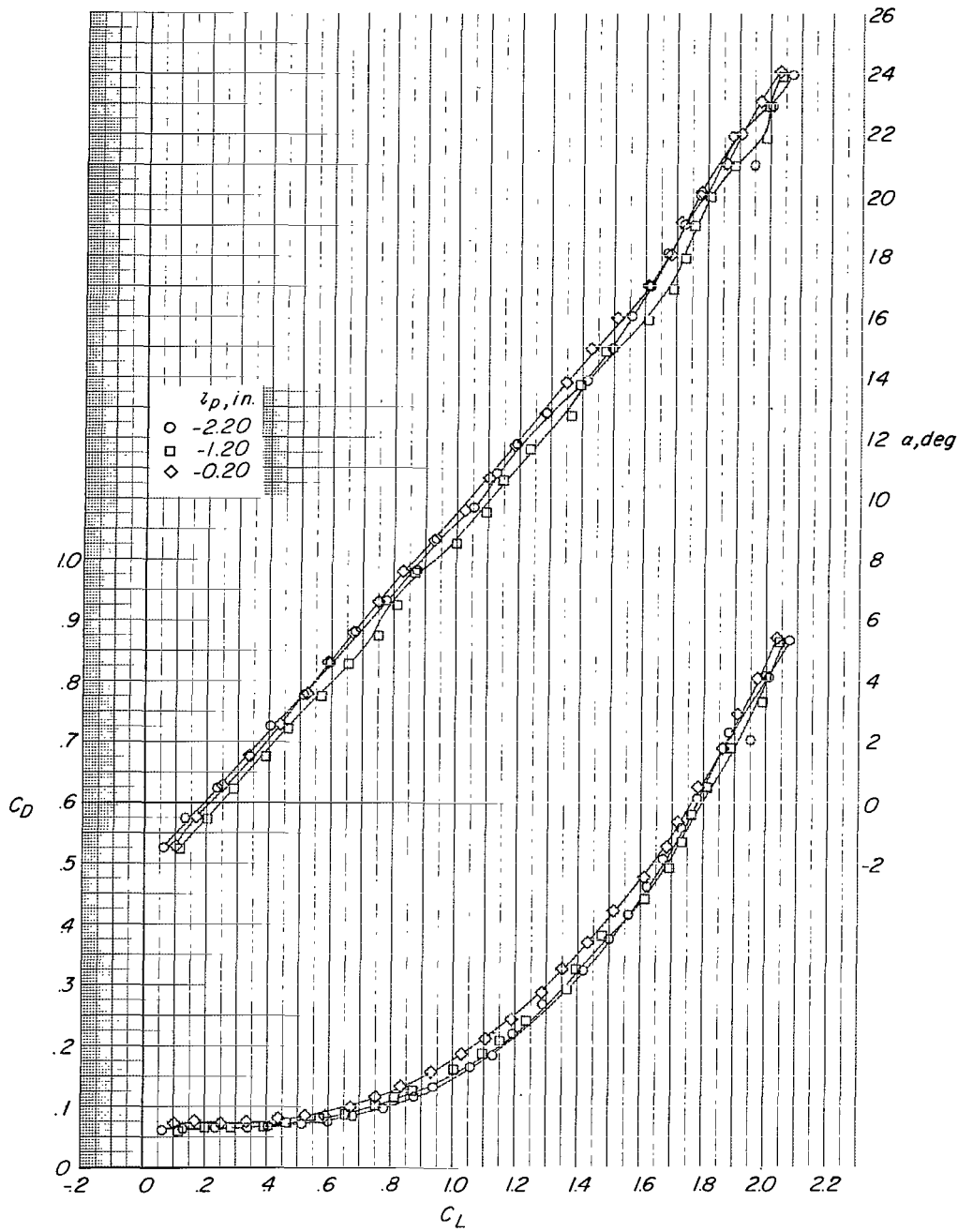


(a) $i_p = 5^\circ$.

Figure 11.- Effect of locating the parawing pivot axis fore and aft of the airplane center of gravity on the longitudinal aerodynamic characteristics for configuration $AP_2$. $h_p = 6.35$ in.; $\delta_t = 0^\circ$.

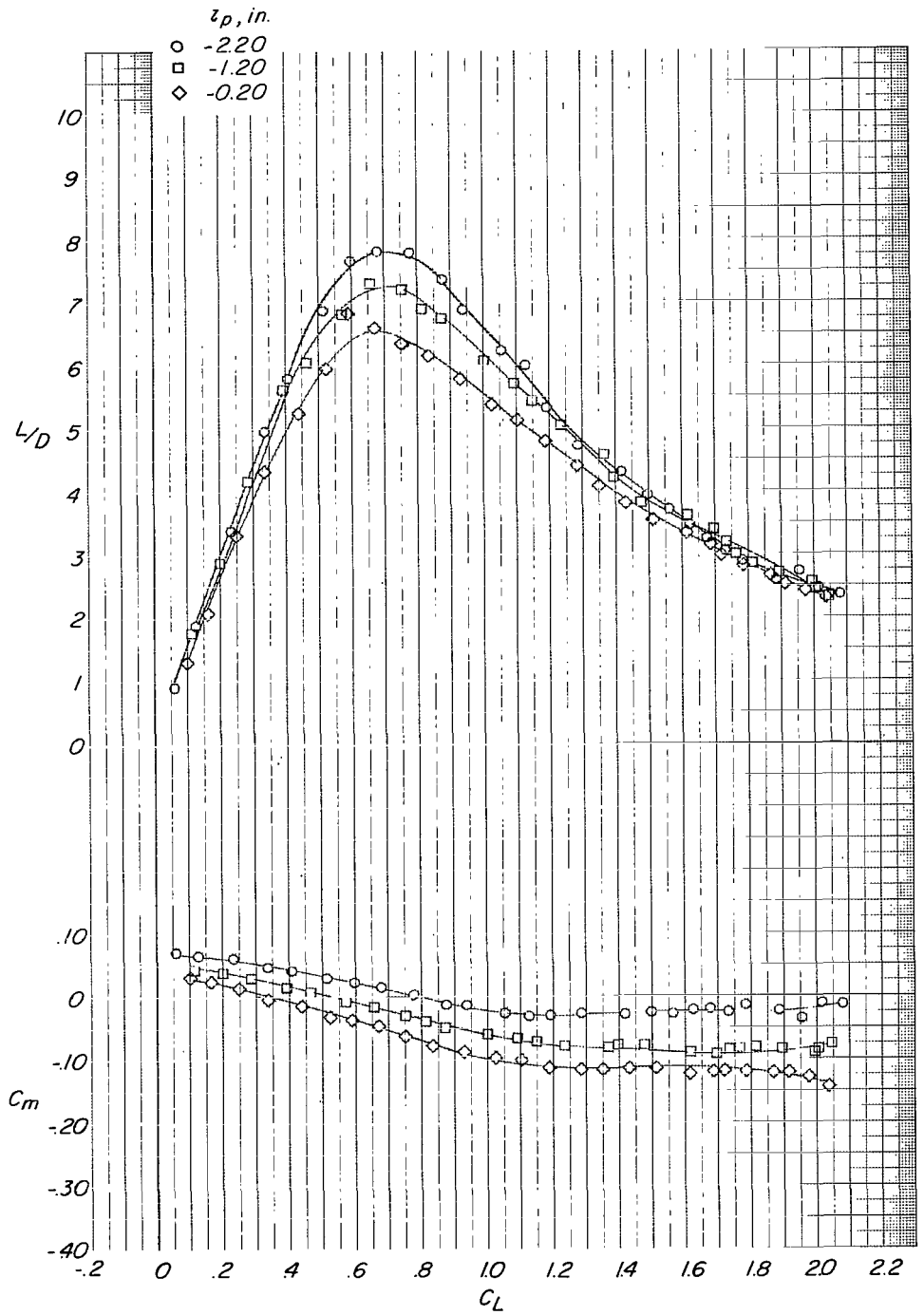


(a) Concluded.

Figure 11.- Continued.

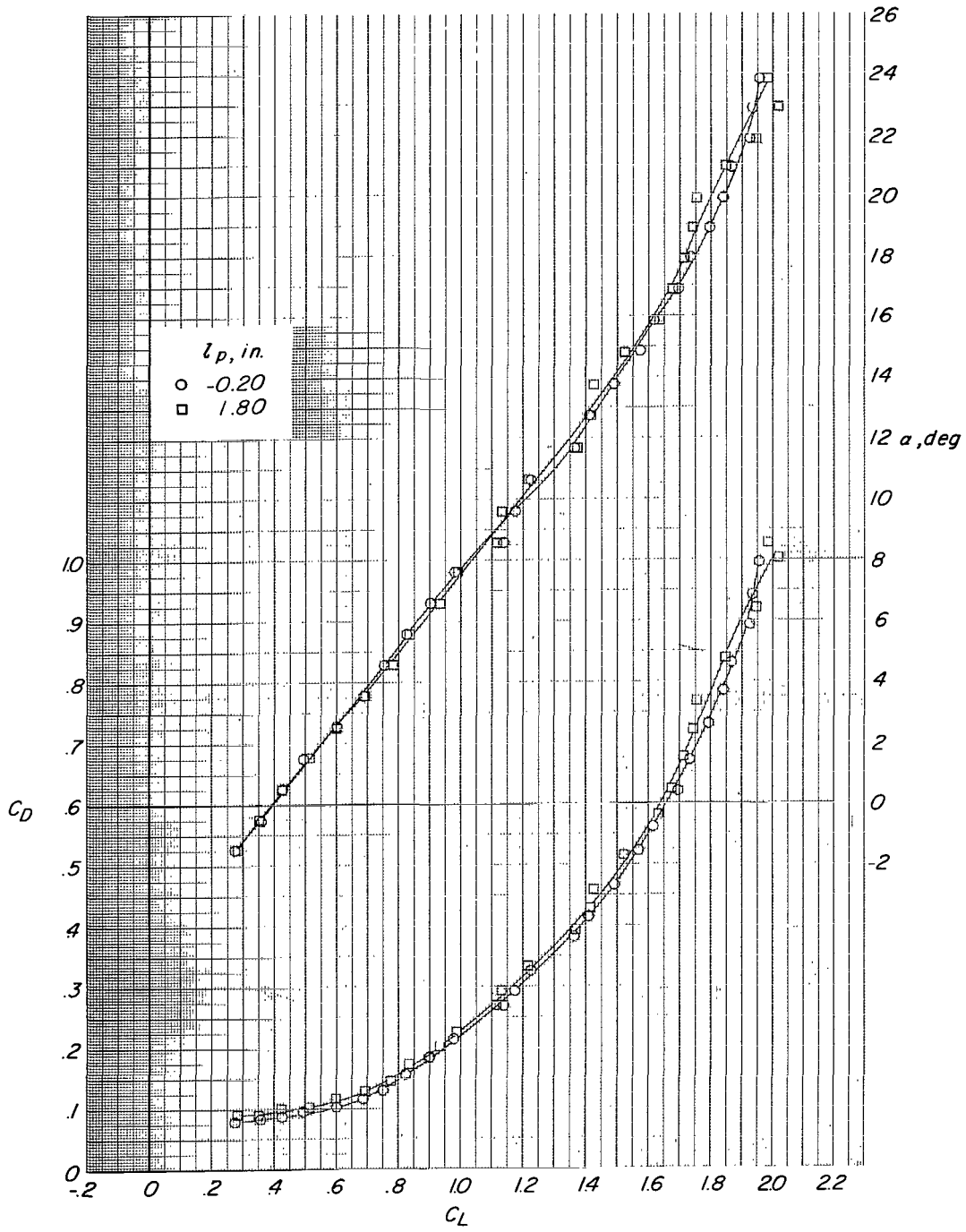


(b) $i_p = 10°$.

Figure 11.- Continued.

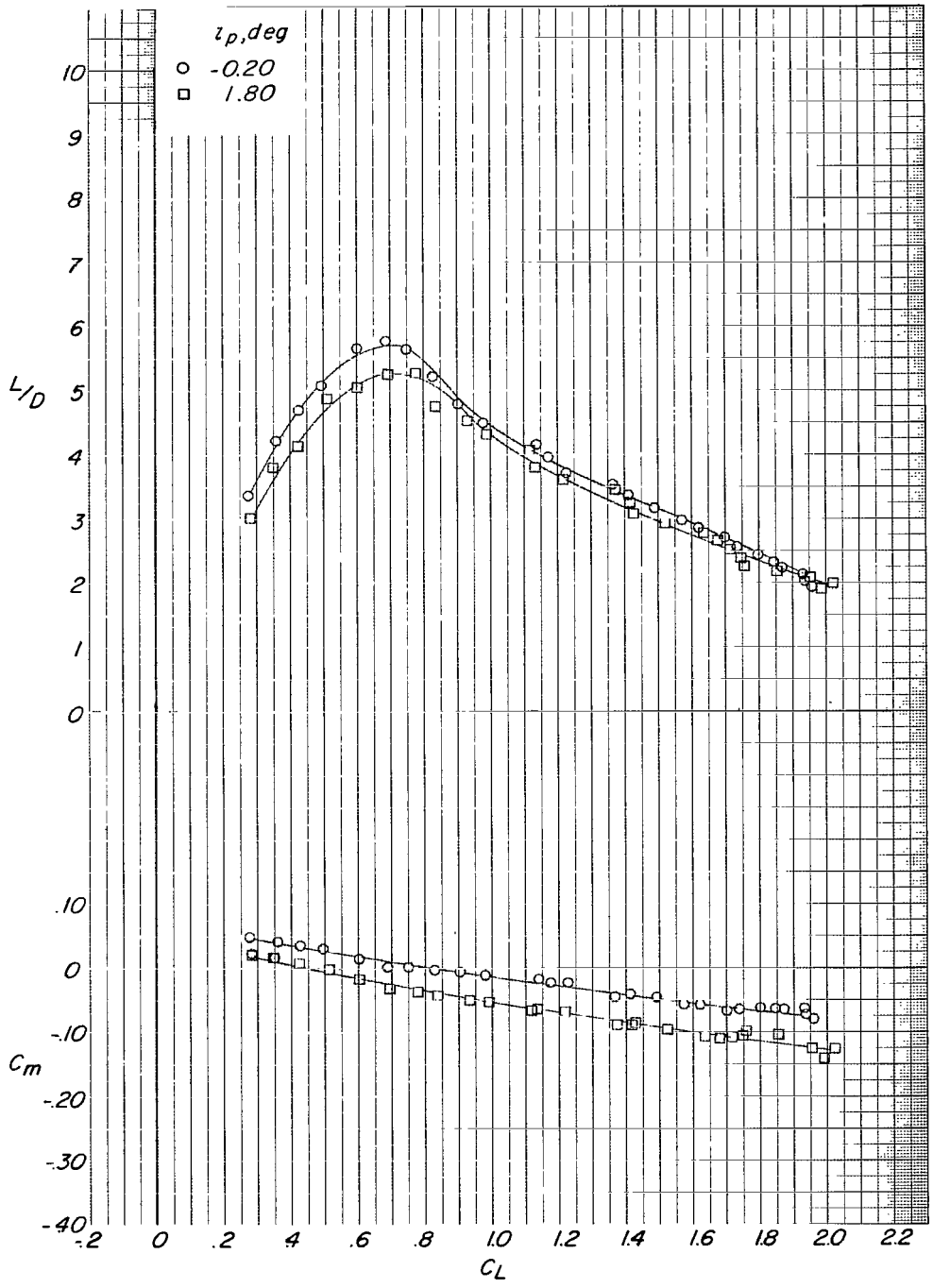


(b) Concluded.

Figure 11.- Concluded.

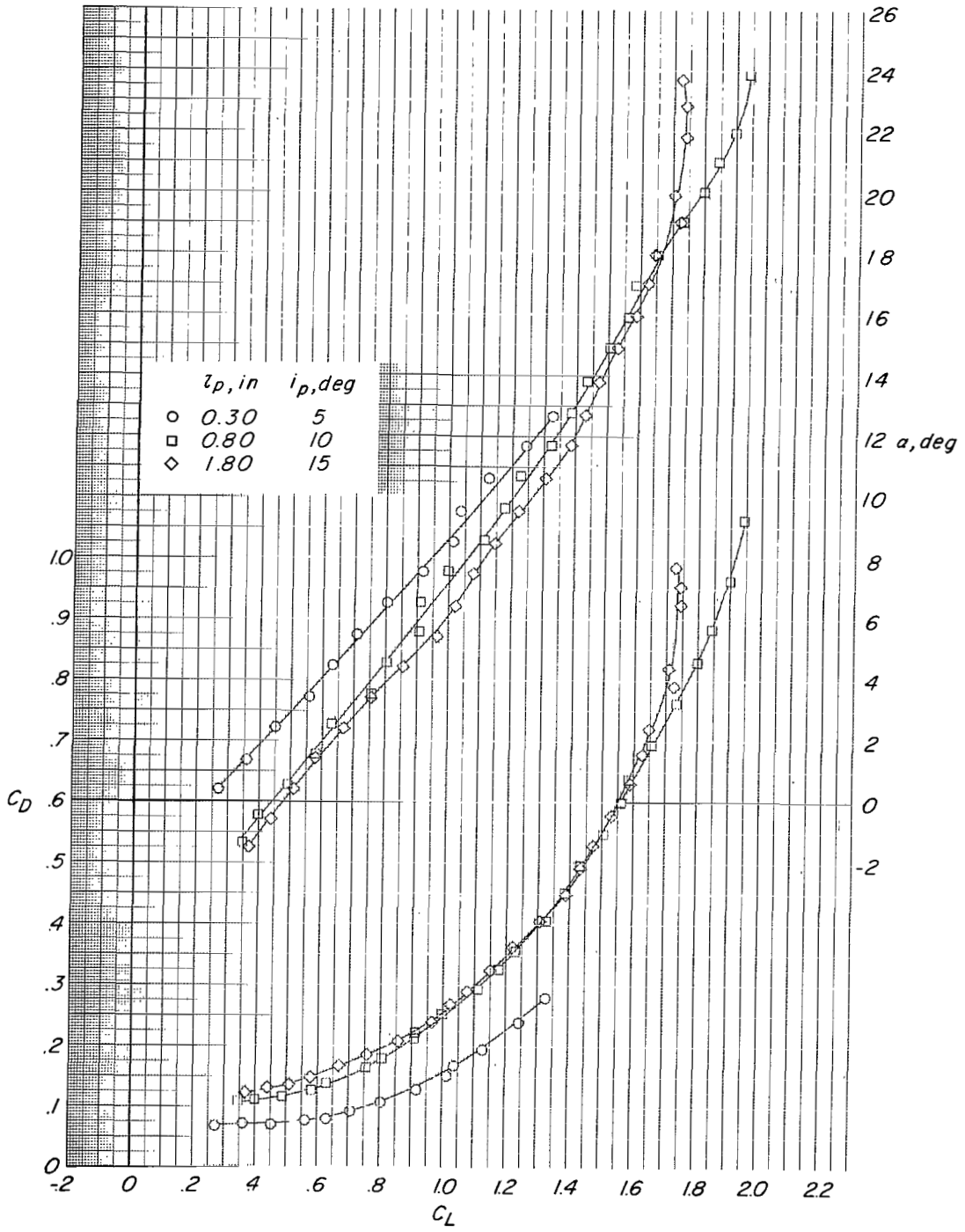


Figure 12.- Longitudinal aerodynamic characteristics of the wire-supported rigid leading-edge parawing (configuration $AP_3$). $h_p$ = 6.35 in.; $\delta_t$ = 0°.

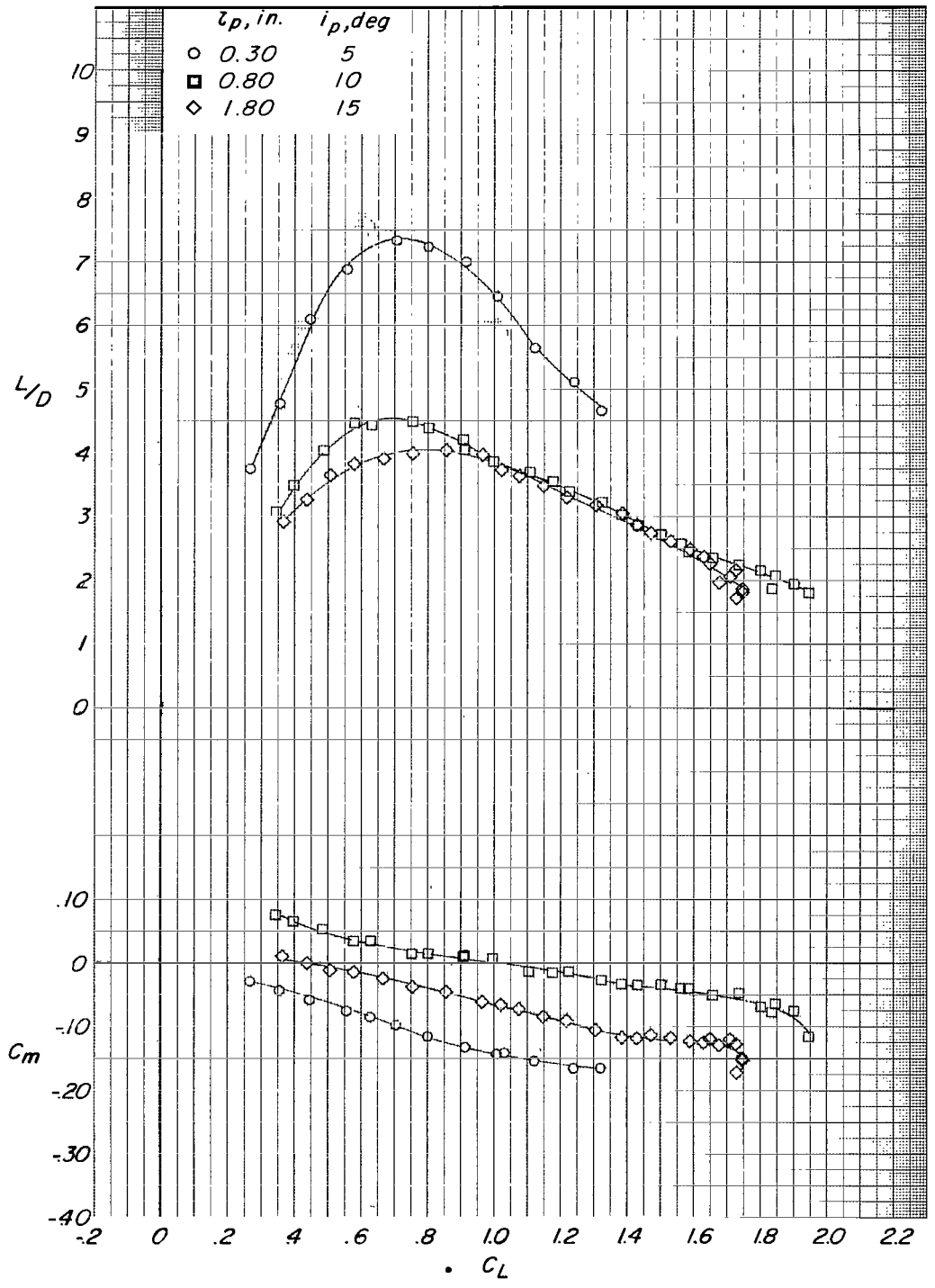


Figure 12.- Concluded.

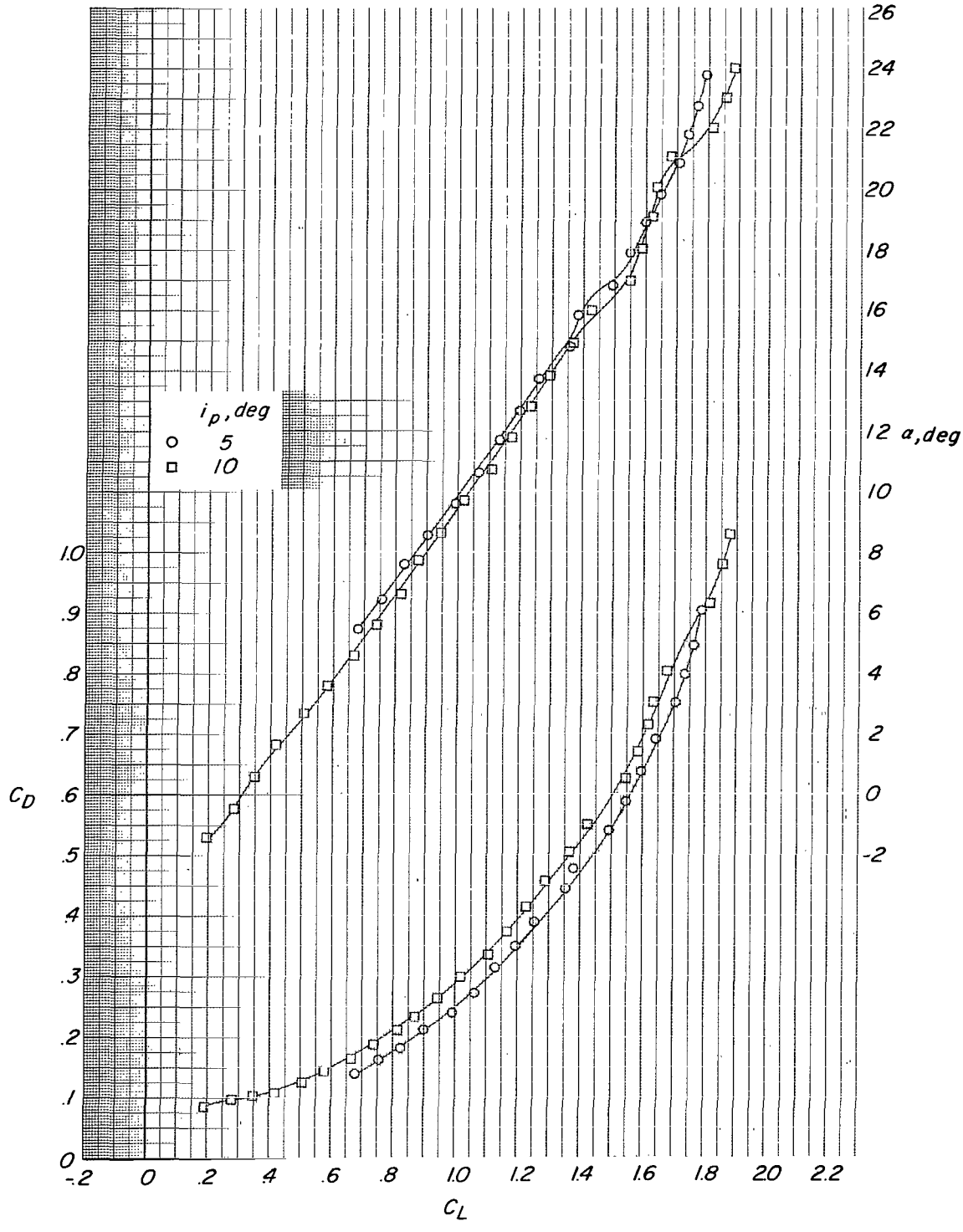


Figure 13.- Effect of parawing keel angle on the longitudinal aerodynamic characteristics for the flexible leading-edge parawing (parawing $AP_4$). $h_p$ = 3.70 in.; $l_p$ = -1.20 in.; $\delta_t = 0^o$.

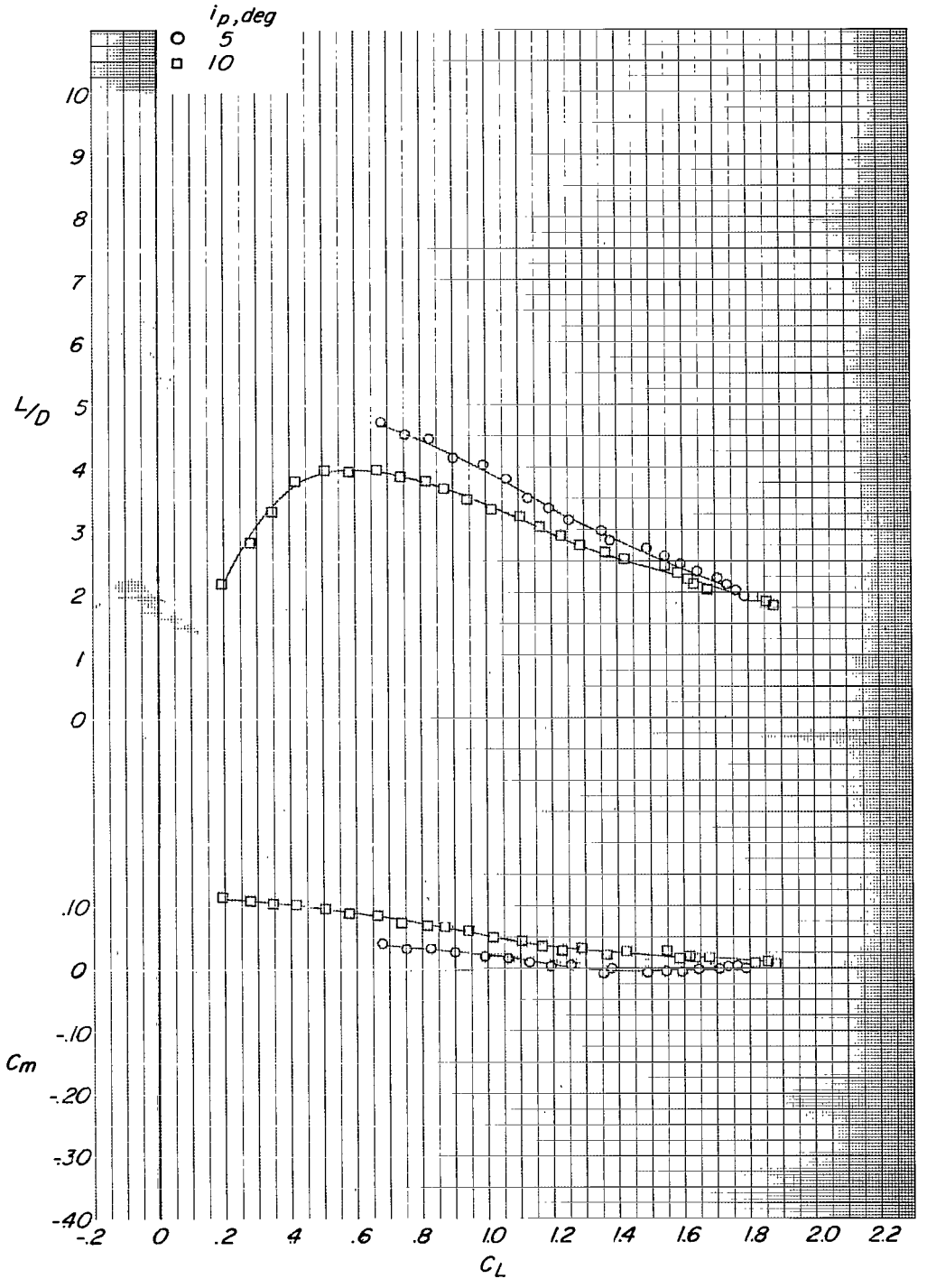


Figure 13.- Concluded.

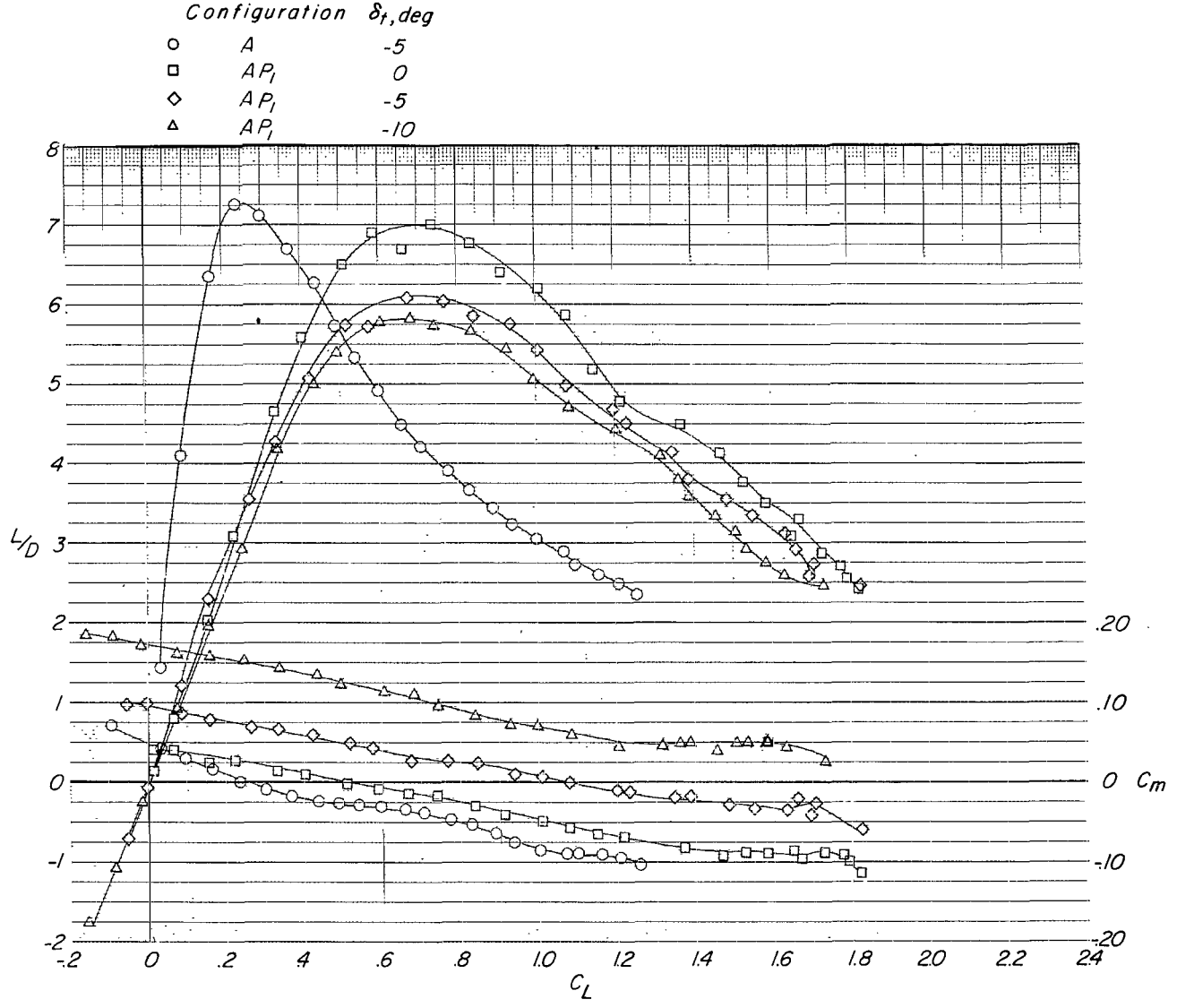


Figure 14.- Effect of horizontal-tail deflection on the longitudinal trim characteristics for configurations A and $AP_1$. $h_p$ = 1.38 in.; $l_p$ = -2.20 in.; $i_p$ = 5°.

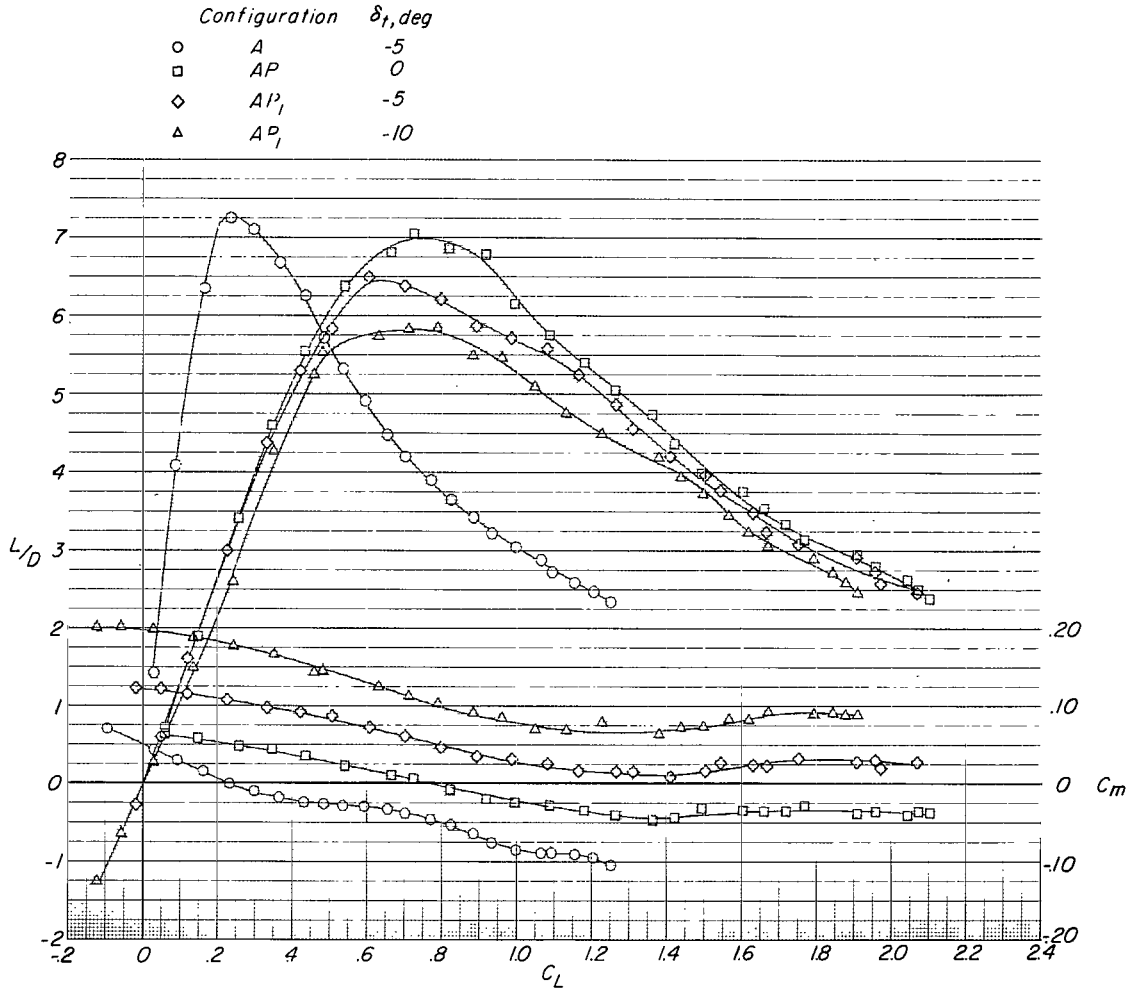


(a) $l_p$ = -2.20 in.; $i_p$ = 5°.

Figure 15.- Effect of horizontal-tail deflection on the longitudinal trim characteristics for configurations A and $AP_1$. $h_p$ = 6.35 in.

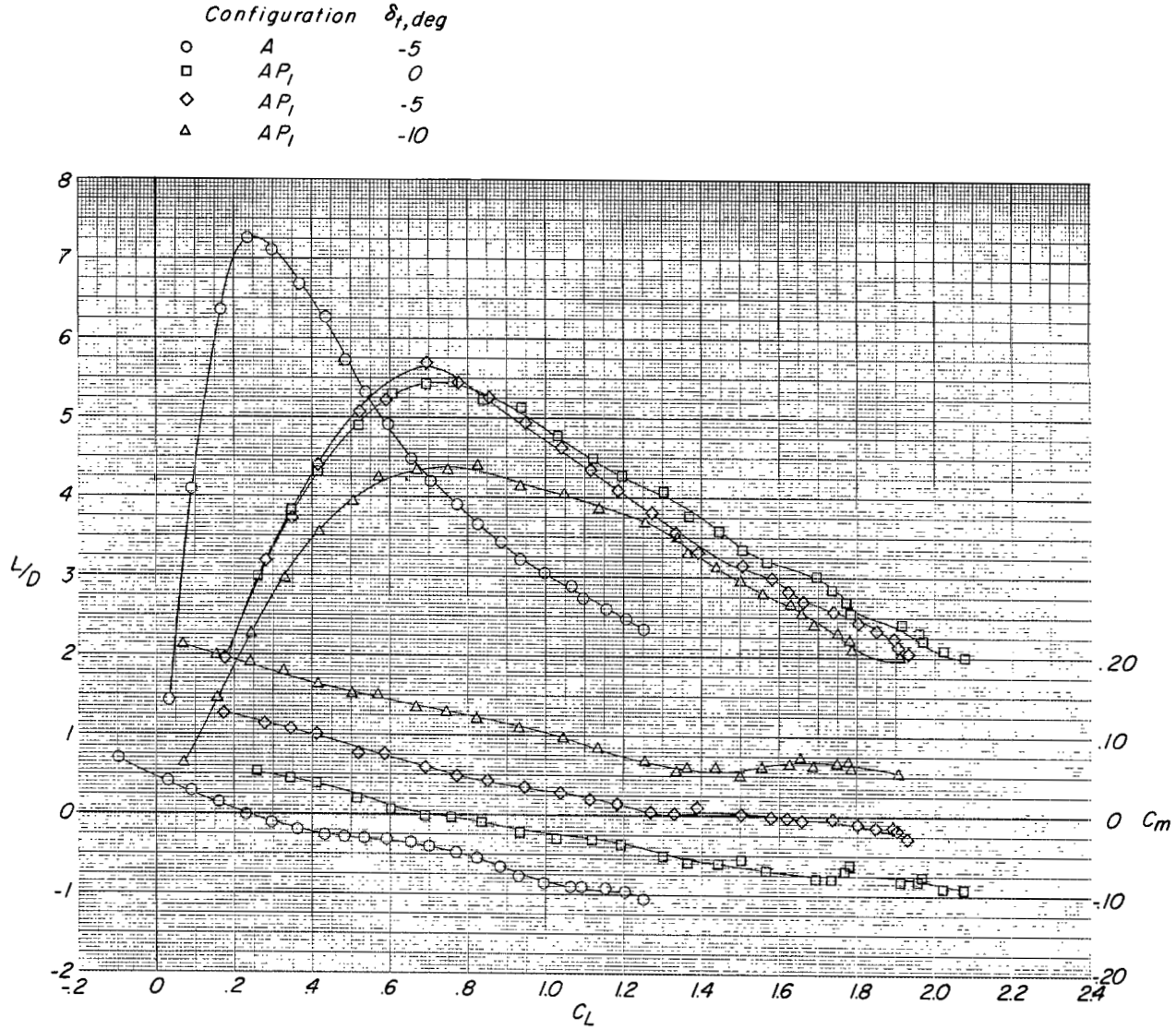


(b) $l_p$ = -0.20 in.; $i_p$ = 10°.

Figure 15.- Concluded.

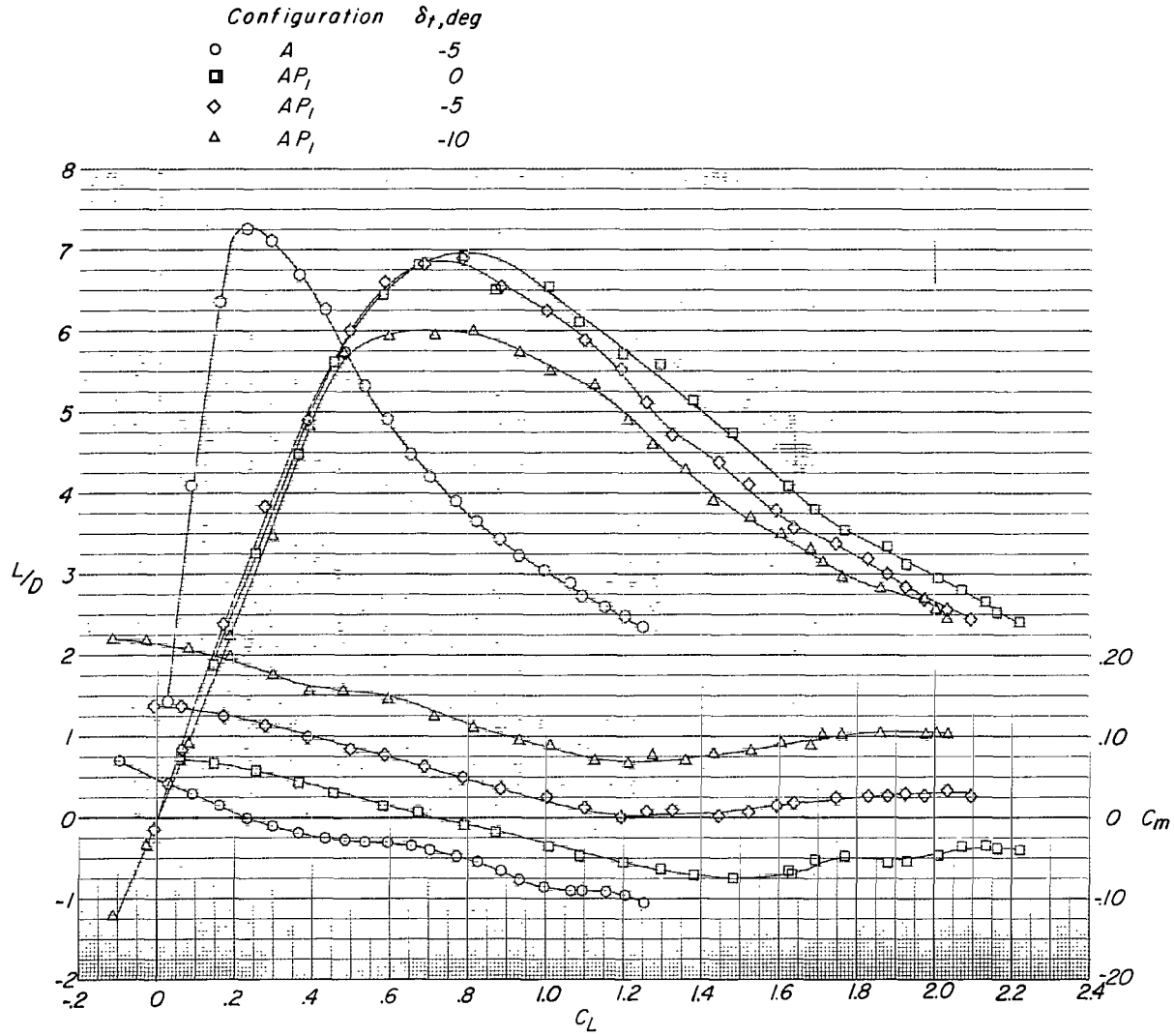


(a) $l_p$ = -2.20 in.; $i_p$ = 5°.

Figure 16.- Effect of horizontal-tail deflection on the longitudinal trim characteristics for configurations A and $AP_1$. $h_p$ = 11.05 in.

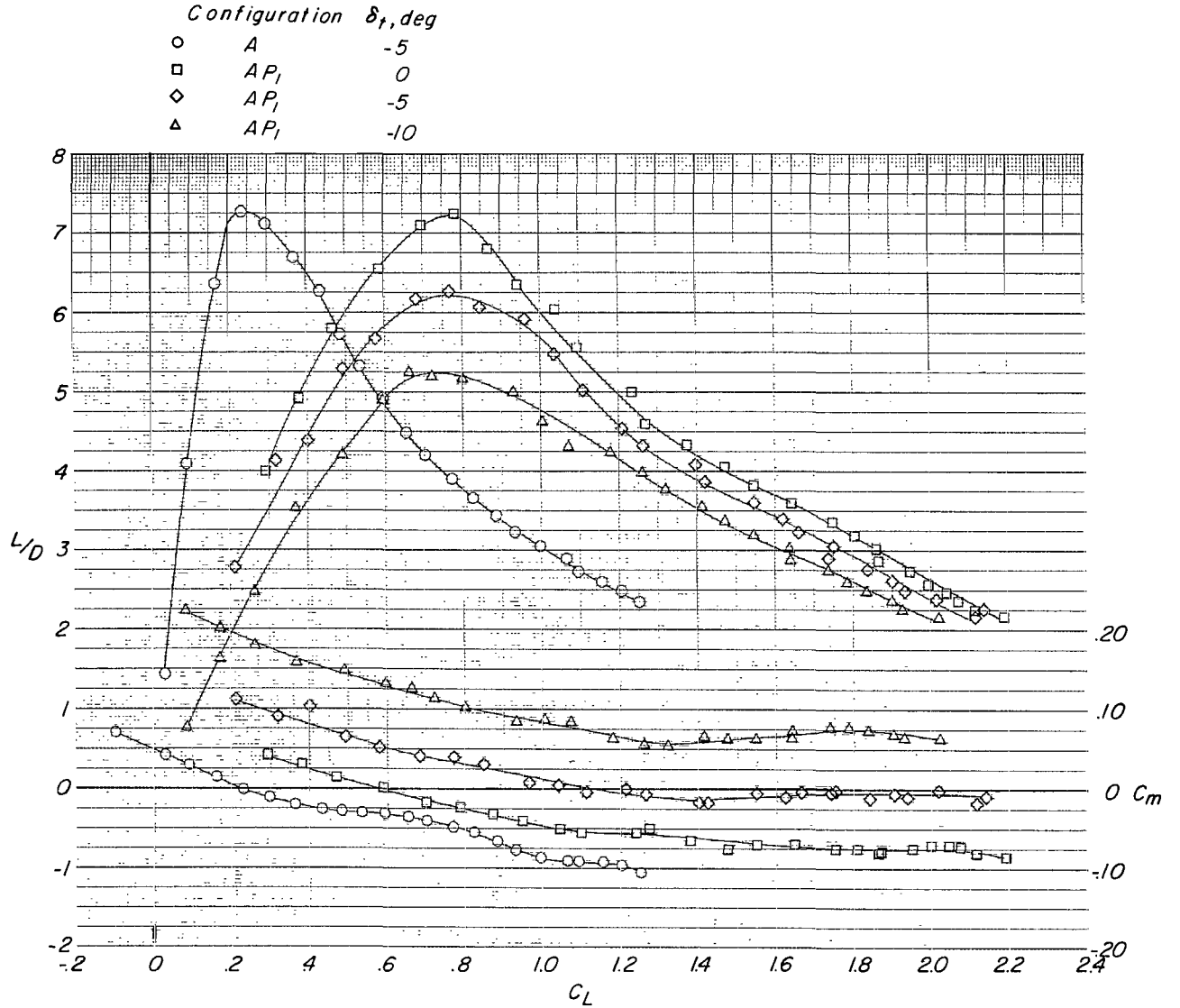


(b) $l_p$ = -0.20 in.; $i_p$ = 10°.

Figure 16.- Concluded.

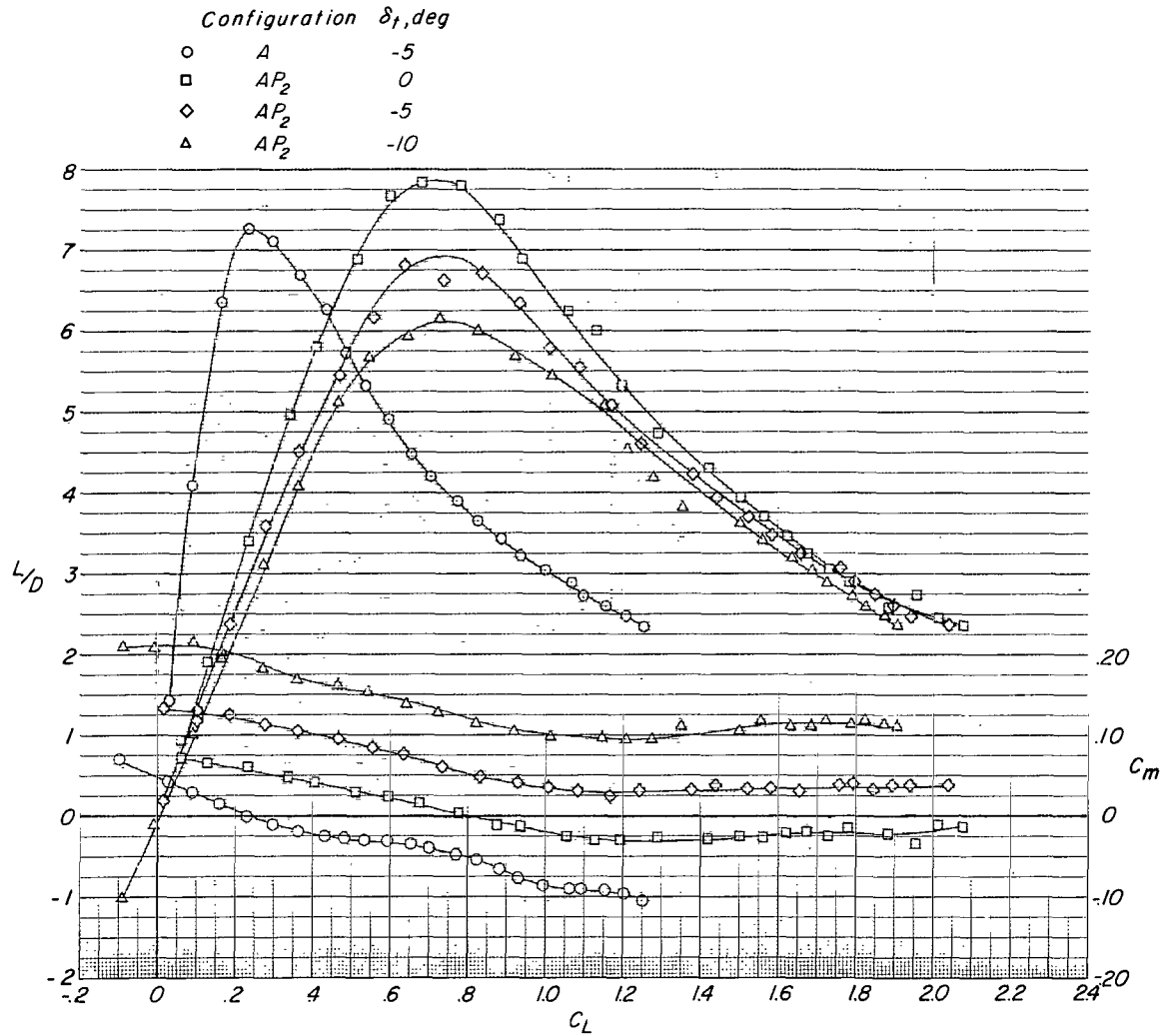


(a) $l_p$ = -2.20 in.; $i_p$ = 5°.

Figure 17.- Effect of horizontal-tail deflection on the longitudinal trim characteristics for configurations A and $AP_2$. $h_p$ = 6.35 in.

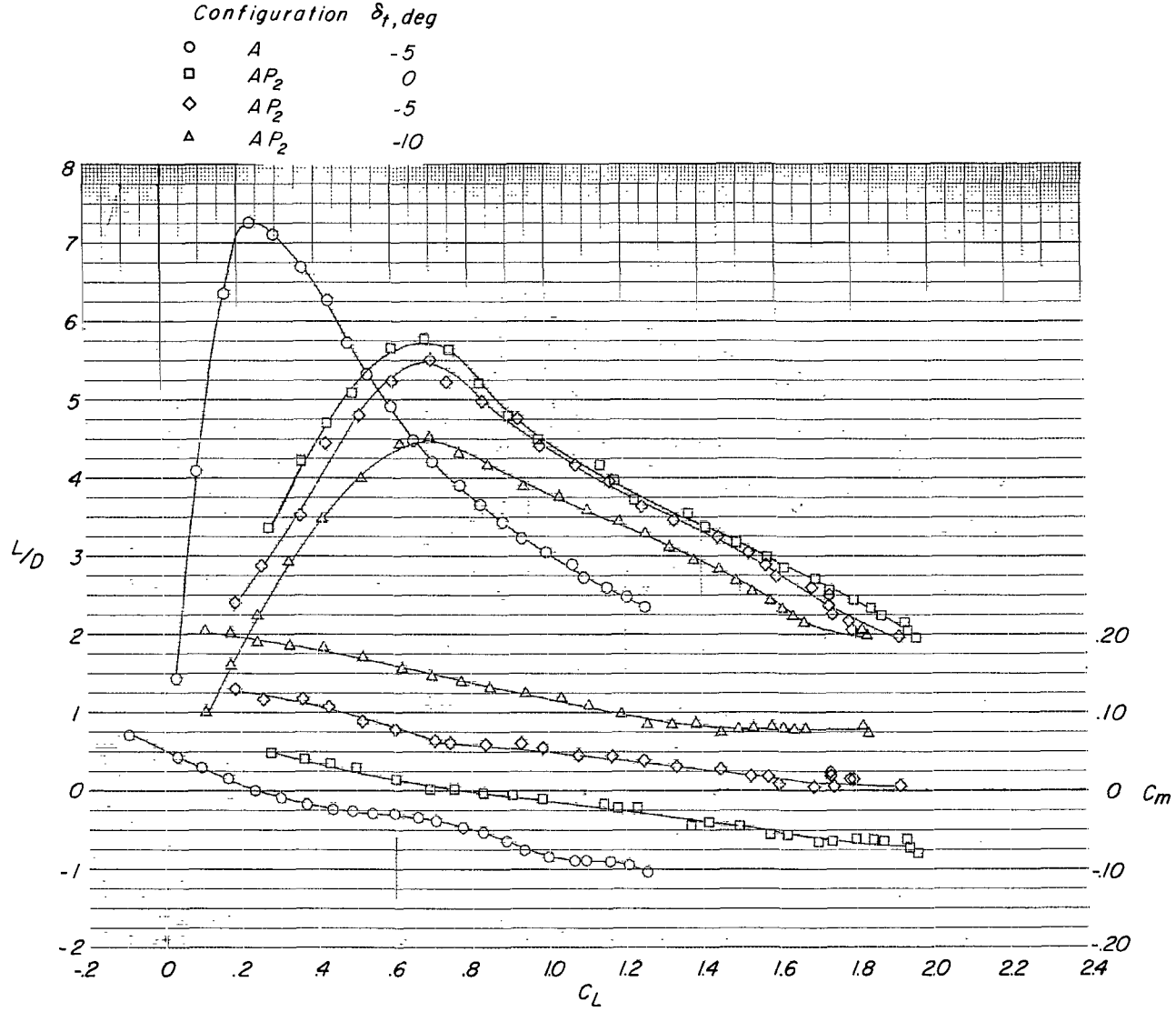


(b) $l_p$ = -0.20 in.; $i_p$ = 10°.

Figure 17.- Concluded.

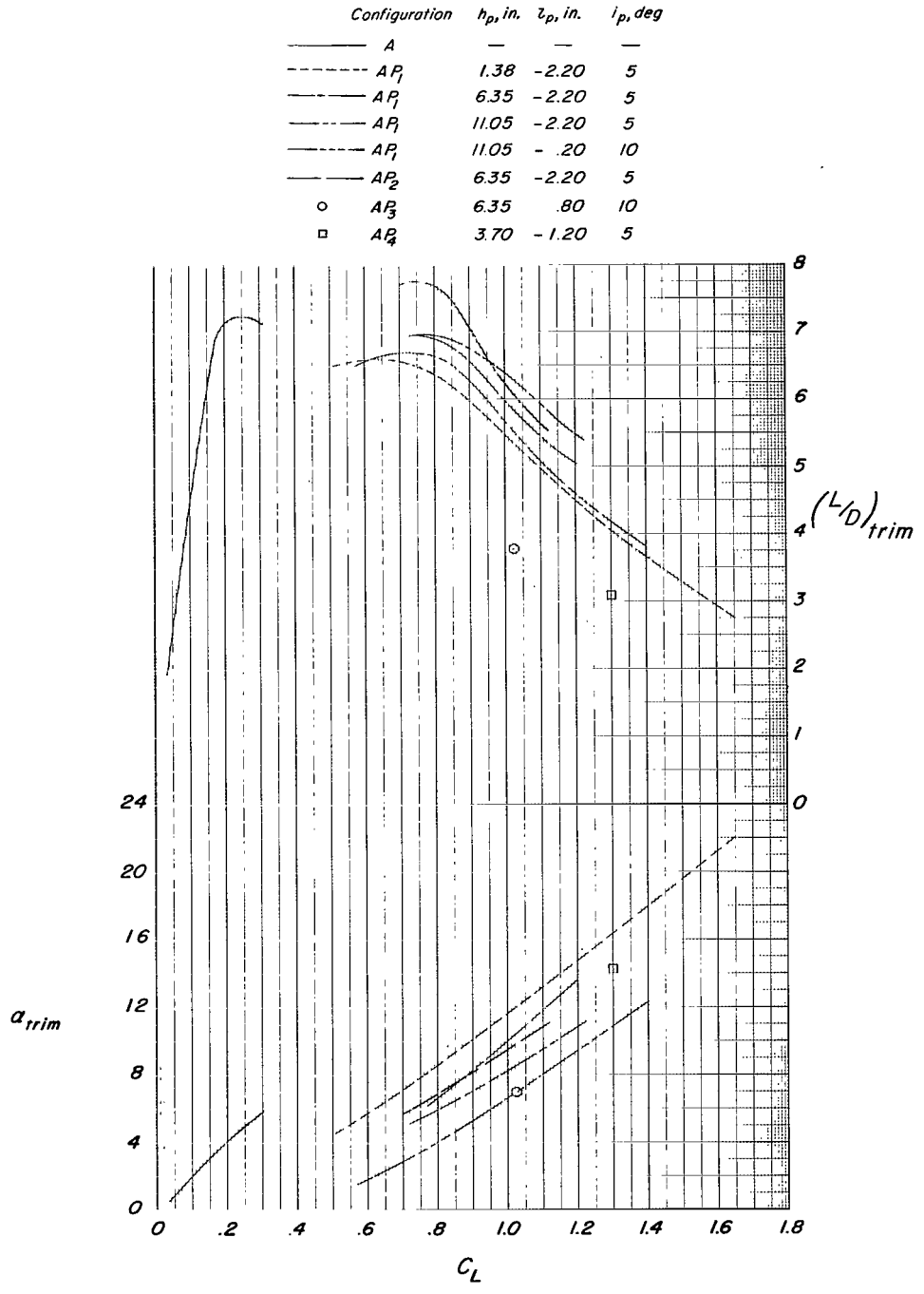


Figure 18.- Variation of the trimmed lift, associated angle of attack, and lift-drag ratio for the airplane alone and the airplane-parawing configurations having the parawing oriented for trimmed conditions at $(L/D)_{max}$ and utilizing variable horizontal-tail deflection.

*"The aeronautical and space activities of the United States shall be conducted so as to contribute . . . to the expansion of human knowledge of phenomena in the atmosphere and space. The Administration shall provide for the widest practicable and appropriate dissemination of information concerning its activities and the results thereof."*

—NATIONAL AERONAUTICS AND SPACE ACT OF 1958

# NASA SCIENTIFIC AND TECHNICAL PUBLICATIONS

TECHNICAL REPORTS: Scientific and technical information considered important, complete, and a lasting contribution to existing knowledge.

TECHNICAL NOTES: Information less broad in scope but nevertheless of importance as a contribution to existing knowledge.

TECHNICAL MEMORANDUMS: Information receiving limited distribution because of preliminary data, security classification, or other reasons.

CONTRACTOR REPORTS: Technical information generated in connection with a NASA contract or grant and released under NASA auspices.

TECHNICAL TRANSLATIONS: Information published in a foreign language considered to merit NASA distribution in English.

TECHNICAL REPRINTS: Information derived from NASA activities and initially published in the form of journal articles.

SPECIAL PUBLICATIONS: Information derived from or of value to NASA activities but not necessarily reporting the results of individual NASA-programmed scientific efforts. Publications include conference proceedings, monographs, data compilations, handbooks, sourcebooks, and special bibliographies.

***Details on the availability of these publications may be obtained from:***

SCIENTIFIC AND TECHNICAL INFORMATION DIVISION

NATIONAL AERONAUTICS AND SPACE ADMINISTRATION

**Washington, D.C. 20546**